Research Square

Preprints are preliminary reports that have not undergone peer review.
They should not be considered conclusive, used to inform clinical practice,
or referenced by the media as validated information.

Effects of Land Cover Change and Climate Variability on the Hydrological Balance of the Kulpawn Basin, Ghana

Osman Zakari
Kwame Nkrumah University of Science and Technology
Charles Gyamfi
Kwame Nkrumah University of Science and Technology
Samuel Ofosu Anim
Koforidua Technical University
E benezer Boakye
Takoradi Technical University
Mabel Kumah
Kwame Nkrumah University of Science and Technology
Kwadwo Asamoa Oku-Afari
Koforidua Technical University
Anornu Kwame Geophrey
Kwame Nkrumah University of Science and Technology
Zakari Osman
osman.zakari@epa.gov.gh

Kwame Nkrumah University of Science and Technology

Research Article

Keywords: Land use-land cover Changes, Climate Variability, Hydrological Processes, Kulpawn River Basin, SWAT Model

Posted Date: July 20th, 2026

DOI: https://doi.org/10.21203/rs.3.rs-10162838/v1

License: This work is licensed under a Creative Commons Attribution 4.0 International License.
Read Full License

Additional Declarations: No competing interests reported.

Effects of Land Cover Change and Climate Variability on the Hydrological Balance of the Kulpawn Basin, Ghana.

Zakari, O[a, b]., Gyamfi, C[a,c], Ofosu, S. A[d]., Boakye, E[e]., Kumah, M[a,f]., Oku-Afari, K. A[d]., Anornu G.K[a,c]

[a] Regional Water and Environmental Sanitation Centre, Kumasi (RWESCK), Kwame Nkrumah University of Science and Technology, Kumasi, Ghana

[b] Environmental Protection Authority, Savannah Region, Ghana

[c] Department of Civil Engineering, Kwame Nkrumah University of Science and Technology, Kumasi, Ghana

[d] Department of Civil Engineering, Koforidua Technical University, Koforidua, Ghana

[e]Department of Civil Engineering, Takoradi Technical University, Takoradi, Ghana

[f] International Water Management Institute, Accra, Ghana

Corresponding Author: Zakari Osman, email: ozakari82@gmail.com; ***tel: +233243924039***

Abstract

Land use and land cover (LULC) changes and variability in climate are critical factors impacting the response and feedback mechanisms of river basins. This work seeks to assess the effects of LULC changes and climate variability on the hydrological conditions of the Kulpawn River Basin (KRB) in Ghana. The study applied the Random Forest (RF) algorithm to classify LULC changes using Landsat images from 1995, 2005, 2015, and 2023. The Soil and Water Assessment Tool (SWAT) was used to analyse the hydro-climatic conditions of the basin. The results revealed substantial conversion of dense savannah forest to built-up areas by 28.34%, light savannah forest by 20.83%, and agricultural land by 3.22%. Significant changes were also observed in key hydrological components, with precipitation decreasing by 2.14% and evapotranspiration by 4.91%, while surface runoff increased by 7.78%. In addition, water yield, lateral flow, and percolation declined by 14.5%, 1.8%, and 4.87%, from 1995 to 2023, indicating reduced water availability in the basin. The study established a strong correlation between LULC changes and hydro-climatic variables of the basin, which highlighted the combined effects of LULC changes and climate variability on basin hydrology. The study recommends the implementation of sustainable land and water use planning and the promotion of climate-smart agricultural practices, as well as the integration of climate adaptation strategies into basin-scale water resources management to enhance the hydrological resilience of the basin.

Keywords: Land use-land cover Changes; Climate Variability; Hydrological Processes; Kulpawn River Basin; SWAT Model

1.0 Introduction

Land use and land cover changes **(**LULC) and climate change (CC) have been recognized as the key drivers of watershed ecology (Aragaw et al., 2022). These global environmental issues have serious consequences on the environment and human systems (Mekonnen and Manderso, 2023). LULC changes driven by rapid urbanization, agricultural expansion, deforestation, and industrialization have impacted various hydrological components, which have resulted in reduced streamflow and surface runoff, reduced groundwater recharge, water yield, and evapotranspiration (Aragaw et al., 2022; Baral et al., 2023; Malede et al., 2023; Ougahi et al., 2022). Sambe et al. (2025) revealed that LULC has profound effects on biodiversity, soil degradation, and the water cycle, with an impact on ecosystem services and functions, as well as human well-being. Asante et al.(2022) and Dahan et al. (2023) also reported that communities and households that depend heavily on land resources for their socio-economic and cultural benefits are more vulnerable to the impacts of climate change. These changes have cascading effects on food security and undermine local resilience to climate shocks and degradation (Kouassi et al., 2021; Timilsina et al., 2023).

The manifestation of climate change presents diverse impacts across landscapes (Adzawla et al., 2020), with rainfall in sub-Saharan Africa expected to be seasonal, with a prolonged dry period (Stewart et al., 2021). Climatic changes cause variations in rainfall and temperature, resulting in hydrological variation (Aragaw et al., 2022). These variations have resulted in low crop yield, adverse health impacts, habitat destruction, and heightened poverty levels among communities and households (Beckline et al., 2025; Liu et al., 2024). These impacts widen the inequality gaps among rural communities that depend on this climate-sensitive resource (Azumah et al., 2021; Murtaza et al., 2023).

Sub-Saharan Africa continues to experience prolonged weather events, with a decrease in surface and underground water resources due to reduced rainfall amount and an increase in evapotranspiration rate (Diba et al., 2018; Kosoe and Ahmed, 2022).

The impacts of LULC and climate change are evident across critical sectors such as agriculture, health, water resources, road infrastructure, and the broader socio-economic landscape (Frimpong et al., 2023; Oti, 2024). These impacts manifest in reduced crop yields, loss of lives

and property, increased flooding and socio-cultural disruptions (Kwawuvi et al., 2022; Murtaza et al., 2023). Among these, the agriculture and water sectors are the most vulnerable to these changes, as extreme temperatures and erratic rainfall patterns continue to undermine agricultural productivity and availability of water resources (Gyimah et al., 2020; Kosoe and Ahmed, 2022).

In Ghana, the savannah ecological zone is considered the most vulnerable region to the impacts of climate change and LULC (Li et al., 2022; Umukiza et al., 2024). This is primarily due to its geographical location and heavy reliance on climate-sensitive sectors for ecosystem services, and for socio- economic, as well as cultural support systems (Issahaku, 2023; Naazie et al., 2023). In addition, the savannah ecological zone is noted for its high temperatures and low rainfall amount. The region is characterized by a single rainfall regime and prolonged dry periods. (Arfasa et al., 2024; Mensah et al., 2022; Nyadzi et al., 2021).

According to Issahaku (2023), temperature and rainfall regimes in Ghana are expected to worsen, with prolonged and severe drought periods and a delay in the onset of rainfall. These events may be characterised by extreme flooding and drought episodes. It is also projected that by 2040, temperature in West Africa, including Ghana, could rise by as much as 6.5 °C under high carbon emission scenarios, significantly exceeding the global mean temperature threshold of 1.5 °C (Kwawuvi et al., 2023). Similarly, Okrah et al. (2020) also projected that temperatures in West Africa and Ghana may increase by 1.5 °C to 3.0 °C by mid-century if current emission trends persist. These projections exceed the global mean target, highlighting the threat climate change poses to Ghana (Ankomah et al., 2021; Baffour et al., 2021). Arfasa et al.(2024) and Naazie et al.(2023) revealed that elevated temperatures in northern Ghana have led to excessive droughts, a decline in soil fertility, and a reduction in soil water retention capacity. These conditions have contributed to a significant decrease in grain and legume production, dropping from 40% to 25% in the last two decades (Fagariba et al., 2018).

Changes in LULC and climate have significantly modified streamflow dynamics, disrupted seasonal water availability, and reduced water quality and ecosystem resilience (Abungba et al., 2022; Tahiru et al., 2020). According to Nyadzi et al. (2021), annual river flows in Ghana declined by 15.00-20.00% in 2020, and are projected to decline further by 30.00-40.00% by 2050 if the prevailing trends in LULC change and climate variability continue.

The White Volta Basin (WVB) is one of the most important river basins in Ghana and contributes significantly to the socio-economic development indices of the country (Osman et

al., 2025). Despite these essential services, the river basin continues to witness sustained decline in its vegetative cover as a result of urbanization, population growth, expansion of croplands, and an increase in the activities of artisanal mining (Nsor et al., 2019; Nyadzi et al., 2021). These activities have severe implications on water availability and quality, with cascading effects on food security, human health, and worsening poverty levels among riparian communities (Bilalam, 2021; Li et al., 2022; Akpoti et al., 2022). Takayama et al.(2023) reported that the incidence of flooding and drought in the river basin is expected to worsen if the current rate of deforestation and unsustainable exploitation of the river catchment remains unchecked. The impacts of these activities could result in the loss of livelihoods and property, a decline in food production, migration, and an economic burden on the public purse (Pabi et al., 2021; Frimpong et al., 2022).

The KRB continues to witness high population growth due to its proximity to urban and peri-urban centres (Osman et al., 2025). This high population growth in the basin increases demand for natural resources, including construction materials and other resources extracted from the river basin (Nyadzi et al., 2021; Li et al., 2022). It is also considered one of the most degraded river basins among the sub-basins of the WVB, and a hotspot for illegal gold mining activities (Mortey et al., 2024; Zakari et al., 2024). Additionally, it is noted for its high agricultural activities, coupled with high volumes of charcoal production and fuelwood extraction (Gross and Pennink, 2018; Adiibokah, 2020). These activities impair the infiltration rate and increase the runoff rate of the basin (Nsor et al., 2019).

The basin is also characterized by high-temperature and unpredictable rainfall regimes with short and high intensity, resulting in perennial flooding and drought (Aabeyir et al., 2024). Adiibokah (2020) and Mensah et al.(2022) further revealed that during the dry season, the basin experiences a shortage of water, resulting in water rationing by the Ghana Water Company Limited. This situation is partly attributed to the inability of the basin to provide the right quantity of water for treatment and supply to communities. The Ghana Statistical Service (2020) also reports that about 60.00% of the population within the basin is engaged in farming activities, of which over 80.00% is rainfed farming. Considering the unpredictability of these hydro-climatic factors in the basin, farming within the basin is becoming very uncertain, with anticipated consequences on food security, land use conflicts, which result in migration, and a decline in ecosystem services (Gross and Pennink, 2018; Nyarko, 2020). It is projected that if the current trend of land cover transition and other climatic factors continues in this manner,

the availability of water in the basin will worsen with severe consequences on the livelihood systems, biodiversity, and ecosystem services (Kranja, 2015; Li et al., 2022).

Addressing these problems will require an integrated approach that establishes the linkages between LULC and the hydro-climatic factors (rainfall and temperature), and their cumulative impacts on the hydrology of the basin. Although previous studies have examined the impacts of LULC and climatic variability in the Nasia and Middle White Basins, these investigations assessed the issues in isolation. For instance, Kumah et al.(2026) and Nyadzi et al. (2021) reported significant climate variability in the Nasia Basin, which was corroborated by Abungba et al. (2022) in the Black Volta Basin, who concluded that LULC changes were more pronounced than climatic factors.

Similarly, Kuma et al. (2021) and Li et al. (2021) also reported that climate change exerts a more substantial pressure on the hydrological system than LULC. However, these studies largely failed to explore the relationships between LULC changes and hydro-climatic variables (rainfall and temperature). In the KRB, there is a noticeable gap with regard to the combined effects of LULC and climate variability in the river basin. The current study seeks to fill this gap by establishing the relationships between LULC changes on temperature and rainfall patterns, and their cumulative impacts on the hydrological processes of the basin. This integrated approach will guide and inform future water resource management strategies in the basin.

In addressing these challenges, the study aims to assess the effects of LULC changes on the hydrological processes and climatic variability in the KRB. The objectives are: to determine the pattern and magnitude of LULC in the basin (1995-2023), assess the effects of LULC on the hydrological processes of the basin, and lastly, assess the trend of rainfall and temperature variability in the basin. The study employed the SWAT model and GIS to simulate and analyze the impacts of LULC on the hydrological and hydro-climatic variables in the basin. Understanding the impacts of LULC and climate variability on the hydrological dynamics of the river basin will ensure management interventions are well targeted and coordinated to mitigate land degradation, ensure water security, and sustainable management practices are not misdirected or become ineffective.

2.0 Materials and Methods

2.1 Description of the study area

The KRB (Figure 1) is one of the sub-basins of the WVB section of Ghana, located at 10.5°N -11.5°N and longitudes 0.5°W -1.5°E. It has a total area of 10,703.7 km². It shares boundaries with other river bodies, such as the Black Volta River Basin to the west, the middle basin of the WVB to the east, the Mole sub-basin to the south, and the Sissili sub-basin to the north (Mensah et al., 2022; Osman et al., 2025). The basin is one of the sub-basins of the WVB, with 70% of it located in the Upper West Region of Ghana (Osman et al., 2025). The river passes through 8 Municipal and District Assemblies (MDAs) in the region.

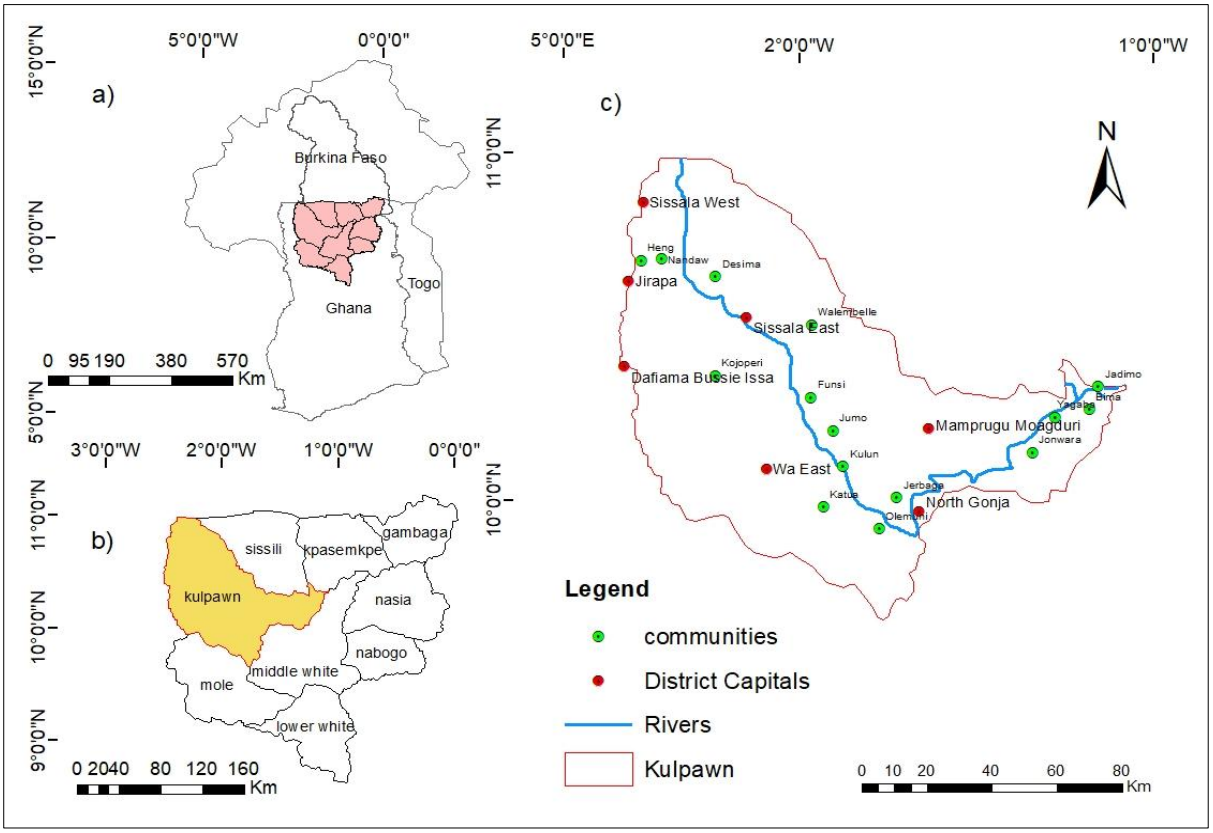


Figure 1. Map of the KRB (a) White Volta Basin, (b) Sub-basins of White Volta Basin in Ghana, (c) KRB

The geology of the basin consists of middle Voltaian rock formation, with a largely flat and undulating terrain suitable for agricultural activities and water supply (Adiibokah, 2020). The predominant vegetation type in the area is the savannah woodlands, characterized by scattered trees and shrubs interspersed with grasses. The common tree species in the basin are the shea (*Vitellaria paradoxa*), baobab (*Adansonia digitata*), dawadawa (*Parkia biglobosa*), and mahogany (*Khaya senegalensis*). These tree species are resistant to the annual bushfires and have economic values that support local economies in the area (Mustapha et al., 2016; Osman et al., 2025). The basin is characterized by a single rainfall regime, which usually begins from

July to September, with an intensity of 800mm-1200mm (Mensah et al., 2022). The intensity varies depending on the specific section of the basin. The high intensities of the rains often result in flooding along the riverbanks (Gross and Pennink, 2018). Additionally, the basin is also characterized by a prolonged dry season with high temperatures of 30 ^{0}C- 40 ^{0}C, occurring between November to April. The basin is an integral part of the drainage network of the WVB system, which comprises various rivers, streams, and tributaries that primarily flow during the rainy season and dry up, or have significantly reduced water volumes in the dry season (Mustapha et al., 2016; Mensah et al., 2022)

The main economic activities in the basin are agriculture with 60.00-70.00% of the population in the basin depending largely on this sector for their socio-economic sustenance (Adiibokah, 2020; Osman et al., 2025). The soil is fertile and supports the cultivation of major crops like maize, millet, sorghum, rice, groundnuts, yams, soybeans, and vegetables. The basin also supports livestock rearing and poultry, as well as small-scale mining and quarrying activities that boost the local economy (Adiibokah, 2020). These activities also contribute to the degradation of the basin as a result of unsustainable practices.

2.2 Data acquisition and processing

2.1.1 Geospatial data

Landsat images for 1995, 2005, 2015, and 2023 were extracted from the United States Geological Survey (USGS) Earth Explorer website (www.earthexplorer.usgs.gov) for the Kulpawn basin. The images (Table 1) for the change detection were selected based on the following criteria:(1) cloud coverage less than 10.00% or cloud-free, and (2) availability of images in a long time series with at least 5-year intervals between images to enhance the differentiation of various land use types (Tan et al., 2015). The selection of the satellite images was carefully done to ensure that the cloud cover was less than 10.00% to enhance the accuracy of the results (Peters, 2019; Tan et al., 2010). The images were pre-processed and cloud cover corrected through a radiometric and atmospheric technique (Fonte et al., 2020; Moisa et al., 2022)

2.1.2 Processing of images

Pre-processing of the Landsat images was done using the Semi-Automatic classification plugin (SCP) in QGIS, while band stacking was performed using the composite bands function in ArcMap 10.6. Image mosaicking and masking were carried out in both ArcGIS and QGIS, and

all datasets were projected onto the WGS 84/UTM Zone 30N coordinate system for consistency and further analysis. Three hundred coordinates were picked using Google Earth for each year group (1995, 2005, 2015, and 2023). These points were used to guide the supervised classification of the pre-processed Landsat images. Five LULC types were identified and used for the classification (Agricultural lands, water bodies, built-up areas, dense savannah forest, and light savannah forest). The selection was based on their dominance in the study area and literature (Table 2). The LULC types identified are considered representative of the broader WVB, including the KRB (Nasare et al., 2023; Nyadzi et al., 2021; Osman et al., 2025)

Table 1. Landsat satellite images used in the study

Satellite	**Sensors**	**Spatial resolution (m)**	**Path/Row**	**Year**	**Cloud cover**
Landsat 5	Thematic Mapper (TM)	30	194/52	1995	4
Landsat 7	Enhanced Thematic Mapper (ETM+)		194/52	2005	1.5
			194/52	2015	0
Landsat 8	Operational Land Images (OLI)		195/54	2023	0

Table 2. LULC classification scheme used for the study

No	**Class**	**Description**	**sub class**	**SWAT LULC Code**	**Description**
1	Dense Savannah	Thick savannah forest	Woodlots, canopy woodlands, sacred groves	FRSD	Forest-Deciduous
2	Light savannah	Light forest	Shrubs, grasses	FRST	Forest-Mixed
3	Water bodies	Area containing water	River, dams. Streams, reservoirs, and marshy areas	WATR	Water
4	Built-up areas	Area covered by settlements and buildings	Residential, commercial, industry, and urban areas	URBN	Residential
5	Agricultural lands	Area under crop cultivation	Croplands, fallow lands, and degraded areas	AGRL	Agricultural lands

2.3. LULC classification and change detection

LULC classification of the KRB was performed using the random forest (RF) machine learning algorithm in R software (R project 2021). The train function in the caret package was used to build the training model. The training samples were grouped into five (5) types: Agricultural lands, built-up areas, dense savannah forest, light savannah forest, and water bodies. The caTools package in R, with the sample split, was used to divide the data into a 70.00% training set and a 30.00% test set. Cross-validation was conducted using K-fold cross-validation. The classification of the LULC types was performed on the pre-processed images. The confusion matrix, Overall Accuracy (OA), and the Kappa coefficient were generated to assess the accuracy of the classification (Savargiv et al., 2021; Amini et al., 2022).

2.2.1 Accuracy assessment

Accuracy of the classified maps was performed using the Kappa coefficient and the overall accuracy (OA) metric (Equations 1 and 2). The kappa coefficient is a widely used accuracy measure in LULC detection analyses, where it reflects the actual agreement of the remotely sensed image with ground-based data (Osman et al., 2025; Sisay et al., 2021).

$$\text{Overall Accuracy (OA)} = \frac{\text{Total number of corectly classified pixel (Diagnonal)}}{\text{Number of Total Reference Pixel}} \times 100 \ldots \text{ equation 1}$$

$$\text{Kappa Coefficient (Ka)} = \frac{T_s \times T_{cs} - \sum(\text{Column total} \times \text{Row Total})}{T_s^2 - \sum(\text{Column total} \times \text{Row Total})} \times 100 \ \ldots\ldots\ldots \text{equation 2}$$

T_s = Total samples and T_{cs} =Total corrected samples (Gautam and Rai, 2022)

The accuracy of the classified maps was assessed and validated using kappa statistics and overall accuracy (OA) metrics for the five land use classes: agricultural lands, built-up areas, dense savannah forest, light savannah forest, and water bodies, for the years 1995, 2005, 2015, and 2023.

2.3 Climate assessment

2.3.1 Climate data

Climate datasets were collected from the Ghana Meteorological Agency (GMET) in Wa, Tumu, and Bolga in the Upper West and Upper East Regions of Ghana, covering the period from 1991 to 2025 for maximum and minimum daily rainfall, temperature, sunshine, wind speed, and

humidity for the KRB. Data were also extracted from the Climate Hazards Group Infrared Precipitation with Station (CHIRPS) to complement the in-situ datasets. Additionally, temperature data was also extracted from the NASA POWER project, using MERRA-2 and GEOS 5.12.4 products (Arfasa et al., 2024). The selection of these satellite data demonstrated a proven ability to accurately reproduce the climatology of the KRB (Nyatuame et al., 2020; Arfasa et al., 2024). Quality control checks from climate station revealed less than 5.0% missing data for both rainfall and temperature.

2.3.2 Global climate models (GCMs) and climate projections

To analyse the suitability of the Global Climate Model (GCM) for the assessment of future climate impacts, vulnerabilities, adaptation, and mitigation strategies, a set of scenarios known as Shared Socioeconomic Pathways (SSPs) has been developed. A set of scenarios known as Shared Socioeconomic Pathways (SSPs) has been developed. These scenarios, as outlined in the IPCC Sixth Assessment Report (AR6), provide five emission scenarios: SSP1-1.9 (very low), SSP1-2.6 (low), SSP2-4.5 (moderate), SSP3-7.0 (high), and SSP5-8.5 (very high) (Aladejana et al., 2018; Kenea et al., 2021). In this study, climate projections for the KRB were carried out using six Global Climate Models (GCMs) from the Coupled Model Intercomparison Project Phase 6 (CMIP6) under two emission scenarios: SSP1-2.6 and SSP5-8.5 for the period of 1995-2023. SSP1-2.6 assumes low emissions driven by improved education, economic growth, and decline population growth, while SSP5-8.5 represents a high-emission future characterized by rapid population growth, economic expansion, and continued dependence on fossil fuels. The selected GCMs, MPI-ESM2-LM, CanESM5, and NorESM2-LM, were based on their proven performance in similar studies conducted in the White Volta, Pra, and Densu Basins (Nsiah et al., 2021; Dzebre et al., 2024; Yenibehit et al., 2024).

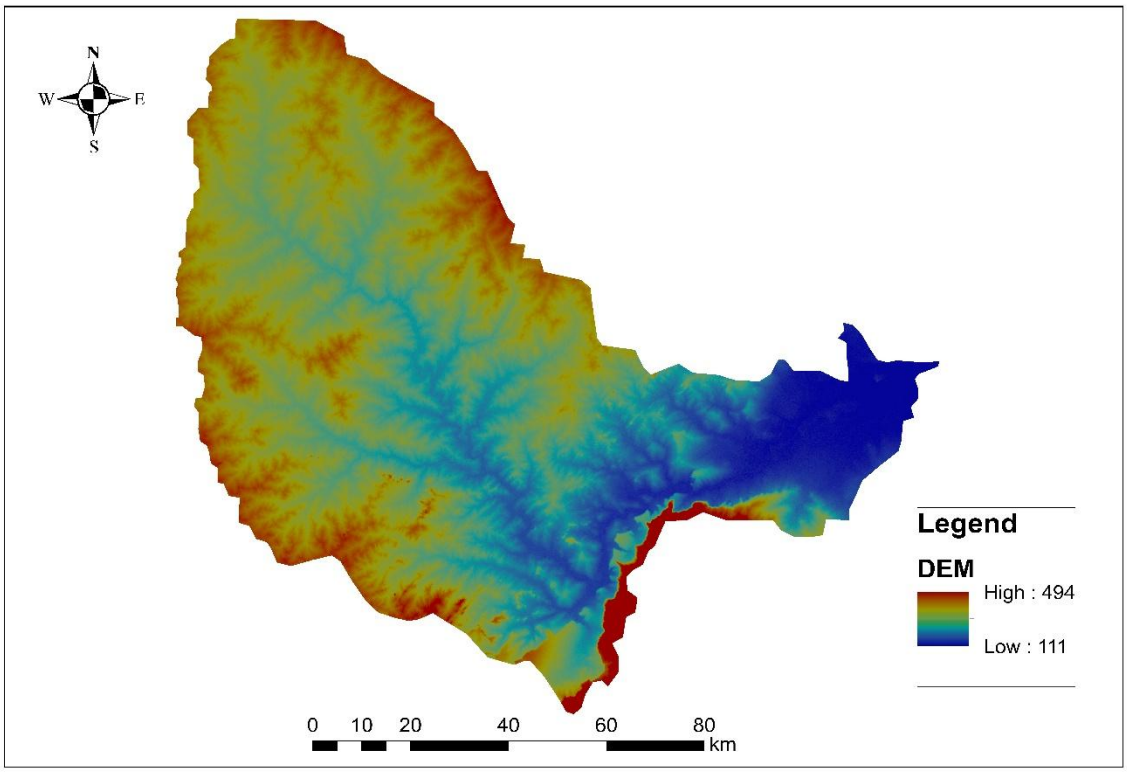
2.3.3 Downscaling GCM data and bias correction

The climate dataset for the basin was downloaded from NASA Earth Exchange Global Daily Downscaled Projections (NEX-GDDP CMIP6) https://www.nccs.nasa.gov/services/data-collections/land-based-products/nex-gddp-cmip6. This is a global downscaled climate scenario derived from the GCM under the CMIP6, which were ran across all greenhouse gas emissions scenarios known as SSPs (Thrasher et al., 2022). The CMIP6 GCMs were designed with respect to the IPCC Sixth Assessment Report (IPCC AR6). This dataset includes downscaled projections from the Scenario Intercomparison Project Model (MIP), which provides a set of global, high-resolution, bias-corrected climate change projections that can be used to evaluate

283 climate change impacts on processes that are sensitive to finer-scale climate gradients and the
284 effects of local topography on climate conditions (O'Neill et al., 2021). Also, the bias-
285 correction spatial disaggregation (BCSD) method is specifically designed to address these
286 challenges associated with GCM outputs (O'Neill et al., 2017).

287 **2.4 Digital elevation model (DEM)**

288 The DEM data for the river basin was extracted from the USGS earth explorer
289 (https://earthexplorer.usgs.gov) with a 30m x 30m resolution from the shuttle radar topography
290 mission (SRTM) 1 Arc-Second DEM. The DEM was projected on the Universal Transverse
291 Mercator (UTM) coordinate system using ArcGIS (version 10.7.1), and the watershed was
292 delineated using the ArcSWAT interface. The stream, outlet, and inlet slopes, and flow direction
293 were defined by the DEM, as well as the sub-basin parameters for further hydrological
294 processing (Figure 2).



295

296 **Figure 2. DEM map of the KRB**

2.5 Soil data

Soil data was retrieved from the Food and Agricultural Organization (FAO) portal. The soil database included soil properties such as organic carbon, pH, water storage capacity, soil depth, cation exchange capacity, soil hydrological group, soil texture, Permanent Wilting Point (PWP), total exchangeable nutrients, and bulk density. The soil type found in the basin is presented in Figure 3 with colour codes. As soil data form an integral component of the study, it explains the dynamics of LULC and how it impacts the hydrological components of the watershed (Mengistu et al., 2023).

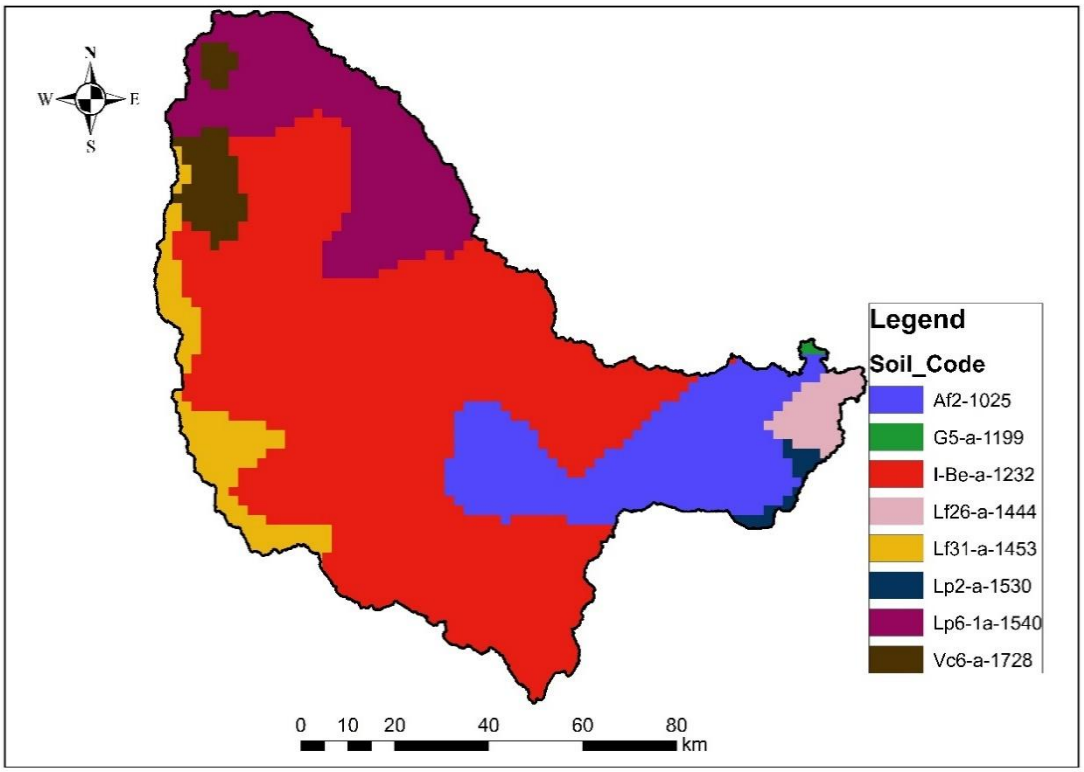


Figure 3. Soil map of the KRB

Table 3. Description of major soil types in the Kulpawn Basin.

No.	Soil codes	Description	Percentages
1	Af2-1025	Ferric Acrisol	15.09
2	G5-a-1199	Gleysol	0.11
3	I-Be-a-1232	Eutric Cambisol	58.35
4	Lf26-a-1444	Luvisols	2.11

5	Lf31-a-1453	Luvisols	5.62
6	Lp2-a-1530	Plinthic Luvisols	0.75
7	Lp6-1a-1540	Plinthic Luvisols	14.74
8	Vc6-a-1728	Chromic Vertisol	3.23

2.6 Application of the soil and water assessment tool (SWAT)

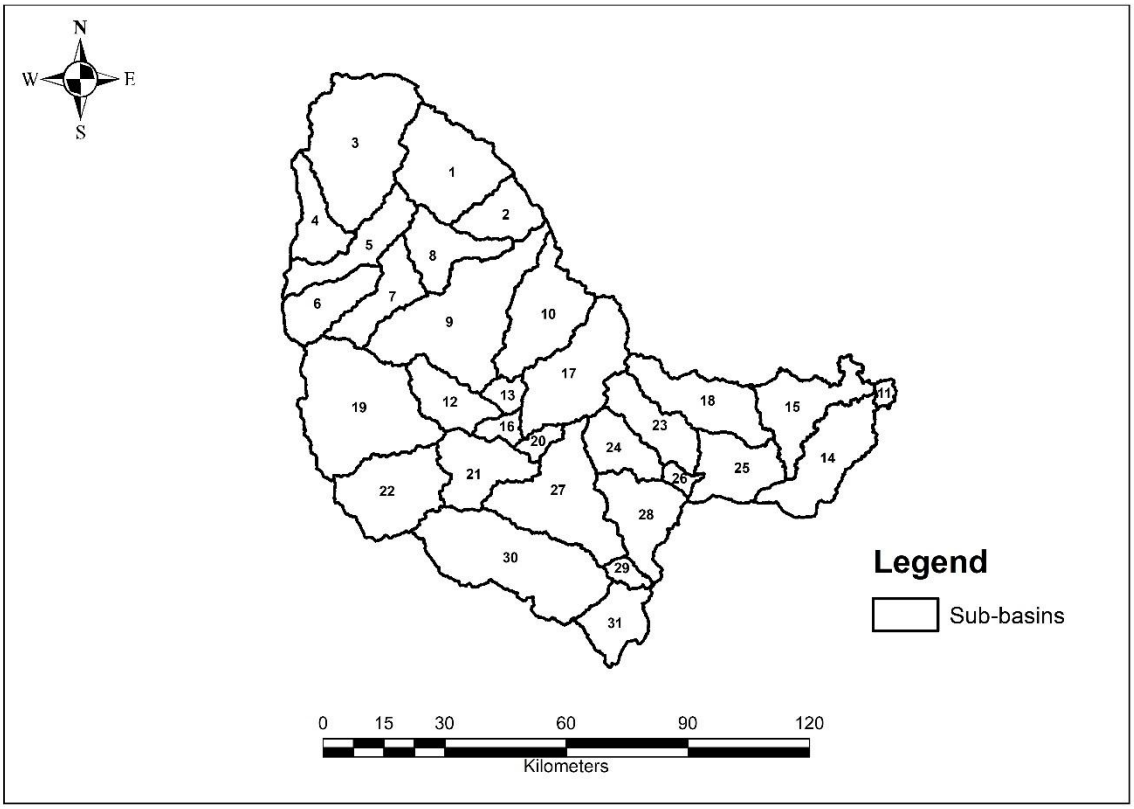
SWAT is an advanced hydrological modelling tool used to simulate the various interactions among watershed, hydrology, soil dynamics, water quality, LULC, and climate processes (Kassaye et al., 2024). One of the key strengths of SWAT is that it can model complex hydrological processes at spatial and temporal scales, making it an ideal tool for studying watersheds and their responses to changing environmental conditions (Emlaei et al., 2022; Arfasa et al., 2024). The SWAT process began with the delineation of the watershed, which involved key stages: DEM setup; stream definition, outlet and inlet definition; selection of watershed outlet (s) set; and the calculation of the sub-basin parameters using the water balance equation (Equation 3)

$$SW_t = SW_O + \sum_{i=r}^{t}(P_{day} - Q_{surf} - ET_P - W_{seep} - Q_{gw}) \quad \text{..... equation 3}$$

SW_t and SW_O = final and initial soil water content; P_{day} = precipitation; Q_{sur} = surface runoff, evapotranspiration; W_{seep} = percolation; Q_{gw}= return flow, all measured in mm (Aladejana et al., 2018; Lukas et al., 2025). The model considers various hydrological components, including precipitation, evapotranspiration, surface runoff, infiltration, groundwater flow, and streamflow, to simulate the movement and fate of water through the watershed (Kassaye et al., 2024; Lukas et al., 2025). SWAT also incorporates climate data, enabling the assessment of climate change impacts on hydrology and water resources by integrating climate projections into the simulations (Malede et al., 2023).

Three model scenarios were performed by the model using different input data: climate data over the baseline period of 1993 – 2014, climate data for the current period 2015 – 2030, and climate data for the future 2031- 2075, using SSP1-2.6 and SSP5-8.5.

The hydrological response units (HRUs) had 114 channels and 31 sub-basins (Figure 4) from the DEM data, of which 10.0% were used for LULC, 20.0% for soil, and 20.0% for slope threshold combinations; each HRU has a unique combination of land use, slope, and soil characteristics.



335

336 **Figure 4. Map of the Kulpawn subbasins**

337 **2.6.1 Simulation and sensitivity analysis of the SWAT model**

338 The SWAT data was simulated using a three-year warm-up period (1990-1992) to normalize
339 the initial conditions and minimize any impact on the model (Idrissou et al., 2022). The
340 simulation was done from 1990 to 2023. The output data were imported into the database, and
341 the streamflow data for the rivers were extracted from the SWAT output table and used for the
342 model calibration.
343 The global sensitivity analysis for SWAT-CUP 2019 was used, simultaneously varying all
344 parameters (Yeneneh et al., 2022). A range of parameters was selected for the sensitivity
345 analysis based on similar studies conducted in different watersheds with similar conditions
346 (Malede et al., 2023). Sixteen (16) variables were selected and used for sensitivity analysis
347 (Table 4), and the level of significance of these parameters were assessed using t-stat and p-
348 value. High absolute value of t-stat depicts strong sensitivity, whiles p-value of zero (0) shows
349 a strong significance level of the parameters (Mengistu et al., 2023). The most significant
350 values are then used for calibration and validation of the model.

351 **Table 4. Flow parameters used for global sensitivity analysis**

No.	Parameter	Description
1	CN2.mgt	SCS runoff curve number
2	ALPHA_BF.gw	Baseflow alpha-factor (days)
3	GW_DELAY.gw	Groundwater delay (days)
4	GMQMN.gw	Threshold water depth in the shallow aquifer (mm)
5	GW_REVAP.gw	Groundwater "revap" coefficient
6	REVAPMN.gw	The threshold water depth in the shallow aquifer for "revap" to occur.
7	SOL_AWC.sol	Available soil water capacity (mm)
8	CH_N2.rte	Manning's "*n*" coefficient for the main channel
9	ESCO.hru	Soil evaporation compensation factor
10	EPCO.hru	Plant uptake compensation factor
11	RCHRG_Dp.gw	DEEP aquifer percolation fraction
12	SL_SUBBSN.hru	Average slope length (m/m)
13	HRU_SLP.hru	Average slope steepness
14	SURLAG.bsn	Surface runoff lag coefficient
15	GW_ SPYLD.gw	Specific yield of the shallow aquifer (m^3/m^3)
16	DEEPST.gw	Initial depth of water in the deep aquifer (mm)

2.6.2 Calibration and validation of the SWAT model

Using SWAT model to assess the impact of climate change and LULC changes , it is essential to perform model calibration and validation to estimate the model parameter values that yield the most accurate hydrological results (Rivas et al., 2022). This is important to maintain the model within a realistic range of uncertainty (Malede et al., 2023). Out of the 62 years (1960 to 2022) of measured streamflow data acquired, 20 years of data (1992-2012) were used for the model calibration and validation, as there was little missing data. The data was divided into two, one for calibration (1992-2001) and the other for validation (2001-2012). Calibration and validation were done with SWAT-CUP 2019 in the sequential uncertainty fittings (SUFI-2). The SUFI-2 produced good accuracy, which represented the observed data with small uncertainties, and required a lower number of iterations to achieve satisfactory results (Kibii et al., 2021; Ngondo et al., 2022).

2.6.3 Evaluation of model performance

The performance of the model was evaluated using data statistical performance indicators; Nash Sutcliffe coefficient (NS), coefficient of determination (R2), and Kling-Gupta Efficiency (KGE) using equations 4, 5, and 6 (Ngondo et al., 2022; Arfasa et al., 2024). The performance of the SWAT, SWAT CUP, and SUFI2 algorithms in uncertain contexts is found on https://swat.tamu.edu/software/swatcup/

$$R^2 = \left(\frac{\sum_{i=1}^{n}(O_i-\bar{O})(P_i-\bar{P})}{\sqrt{\sum_{i=1}^{n}(O_i-\bar{O})^2}\sqrt{\sum_{i=1}^{n}(P_i-\bar{P})^2}} \right), \ldots\ldots\ldots\ldots\ldots\ldots\ldots\ldots\ldots\ldots \text{ ...equation 4}$$

R^2 = the percentage of variation explained by the model. It is a statistical measure of how close the data are to the fitted regression line (Equation 4). O_i = observed variable, P_i = predicted variable, $\bar{P}$ = mean of the predicted variable, $\bar{O}$=mean of the observed variable(Malede et al., 2023).

$$NSE = 1 - \left[\frac{\sum_{i=1}^{n}\left(Y_i^{obs}-Y_i^{sim}\right)^2}{\sum_{i=1}^{n}\left(Y_i^{obs}-Y_i^{mean}\right)^2} \right] \qquad \ldots\ldots\ldots\ldots\ldots\ldots\ldots\ldots\ldots\ldots\ldots\ldots\ldots\ldots\text{equation 5}$$

The NSE quantifies the relative magnitudes of the residual variance (noise) compared to the observed data variance. Y_i^{obs} = sum of observed, Y_i^{sim} = sum of simulated, Y_i^{mean} = mean of the observed (Idrissou et al., 2022; Mekonnen & Manderso, 2023).

Kling-Gupta Efficiency (Gupta *et al.,* 2009) adopted NSE compositions into its components and addressed several shortcomings in NSE (Idrissou et al., 2022; Ngondo et al., 2022).

$$KGE = 1 - \sqrt{(\gamma-1)^2 + (\alpha-1)^2 + (\beta-1)^2} \qquad \ldots\ldots\ldots\ldots\ldots\ldots\text{equation 6}$$

Where $\alpha = \frac{\sigma_s}{\sigma_m}$, $\beta = \frac{\mu_s}{\mu_m}$ and γ is the linear regression coefficient between the simulated and observed variables, $\mu_s$and $\mu_m$are means of simulated and observed data, $\sigma_s$and σ_m are the standard deviations of simulated and observed data.

2.6.4 Scenario-based impact assessment

LULC and climate change scenarios were assessed using appropriate models and approaches, considering the spatial and temporal dynamics of the study area. LULC changes were projected for the years 1995, 2005, 2015, and 2023, while climate change simulations used the same years of 1995, 2005, 2015, and 2023. The model was then utilized to simulate hydrological

components such as potential evapotranspiration (PET), evapotranspiration (ET), surface runoff (SurQ), groundwater flow (GWQ), precipitation (Precip), and water yield (WYLD) using equation 3. The impacts of LULC and climate change were evaluated by comparing monthly, seasonal, and annual outputs from the baseline period with those from individual and combined LULC and climate change scenarios.

2.7 Uncertainty and limitations of the study

One of the challenges of the study was the limited number of meteorological stations within the catchment. This may constrain the accurate representation of the spatial variability of climatic conditions within the watershed. This may affect key model input data, such as precipitation and evapotranspiration (Guug et al., 2020). Although the model may assume uniform climatic conditions across the watershed, this assumption may not hold in reality and is likely to cause significant hydrological variations (Kassaye et al., 2024; Lukas et al., 2025). Although the model may assume uniform climatic conditions across the watershed, this assumption may not hold in reality and is likely to cause significant hydrological variations, given the fact that climate change and LULC are processes that could cumulatively affect the hydrology of the basin (Kenea et al., 2021).

The SWAT model has inherent limitations that lie in the complexity of analysing hydrological processes at the HRU and landscape unit levels (Aragaw et al., 2022). The model simulates processes based on detailed spatial objects such as LULC, soil types, and slope classes. While this object-oriented structure enhances the spatial detail of simulations, it also introduces analytical challenges, making the results more complex to interpret (Malede et al., 2023; Mengistu et al., 2023). Despite its complexity and unsuitability for interpretation, the output is more reliable at the HRU than in the sub-basin. This constitutes one of the drawbacks of the SWAT model.

Despite these challenges, the calibrated SWAT model demonstrated good performance at the monthly scale, providing results that are robust and reliable for assessing the individual and combined impacts of land use and climate change on hydrological processes in the basin.

3.0 Results and Discussion

3.1 Classification and accuracy assessment of LULC maps

LULC analysis of the KRB was performed from 1995 to 2023, and LULC maps generated for 1995, 2005, 2015, and 2023 (Figure 5). The accuracies of the classified maps were determined using Ka and OA for the five land use categories. The accuracies were within the range of 0.68-0.80 for Ka and 79.0%-81.0% for OA (Table 5), which portrayed a good agreement (Arifeen et al., 2021). Higher accuracy values signify good reliability and how accurately the classified maps support further processing and enhanced analysis (Gudmann et al., 2020).

The OA of the classified maps exceeded the minimum threshold value of 80% set for effective LULC, and a Ka close to 1.0 indicated a more accurate result (Minallah et al., 2019; Fonte et al., 2020). The LULC maps of the basin were reliable and could be used for further processing and analysis to support effective decision-making.

Table 5. Accuracy matrix of LULC of the KRB from 1995 to 2023

Years 1995	LULC Type	Agric	Buil up	DF	LF	Water	Total	User Accuracy (%)
	Agric	52	7	0	1	0	53	80
	Built up	0	41	0	0	7	55	75
	DF	0	3	47	0	1	79	69
	LF	0	0	0	50	6	56	79
	Water	5	4	0	0	49	39	88
	Producer Accuracy (%)	68	67	80	83	92		
	OA (%)	**80**					**Ka**	**0.79**
2005	Agric	44	4	0	0	0	43	67
	Built up	0	51	0	0	4	65	75
	DF	0	8	45	0	1	79	59
	LF	0	0	0	50	6	56	89
	Water	4	0	1	0	39	49	78
	Producer Accuracy (%)	84	79	68	78	81		
	OA (%)	**81**					**Ka**	**0.68**
2015	Agric	59	4	0	0	1	51	92
	Built up	1	39	0	0	4	55	75
	DF	0	2	47	0	1	79	59
	LF	3	0	0	50	6	56	89
	Water	12	1	4	3	39	39	83
	Producer Accuracy (%)	92	80	100	92	97		
	OA (%)	**79**					**Ka**	**0.87**
2023	Agric	0	0	1	9	0	50	80
	Built up	0	41	0	0	4	55	75
	DF	0	3	47	0	1	79	61
	LF	0	5	0	44	6	56	87

Water	51	0	3	0	41	49	90
Producer Accuracy (%)	80	67	71	74	80		
OA (%)	**80**					**Ka**	**0.81**

Note: DF=Dense savannah forest: LF=Light savannah forest

3.2 Spatial Patterns and Changes in Land Use/Land Cover Types

The LULC trend in the KRB was assessed from 1995 to 2023 for major LULC types (Figure 5 and Table 6). The pattern and distribution of LULC change in the basin exhibited characteristics similar to those reported in previous studies in the WVB and other parts of northern Ghana (Aabeyir et al., 2024; Nyadzi et al., 2021; Osman et al., 2025).

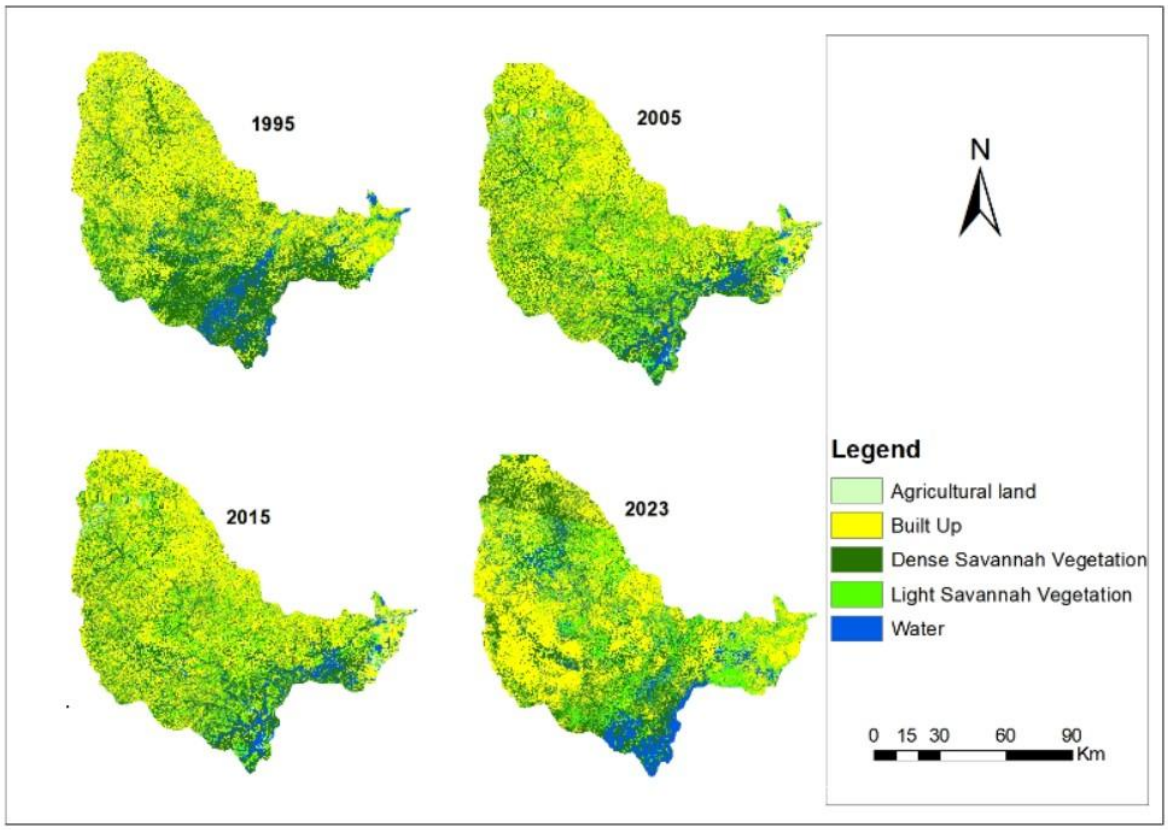


Figure 5. Classified maps of the KRB for 1995, 2005, 2015, and 2023

The spatio-temporal distribution of the LULC types in the basin for the study periods for Agricultural lands exhibited a generally increasing trend with an annual rate of 9.35% across the basin. This increase in agricultural lands may be attributed to an increase in agricultural activities, as a result of the agrarian nature of the basin (Osman et al., 2025). It is reported that 60.0-70.0% of inhabitants derive their livelihoods from agricultural activities (Adiibokah,

2020; Ghana Statistical Services, 2021). This may also be coupled with the high human population density in the basin (Aabeyir et al., 2024).

Built-up areas witnessed an increased pattern of 29.80% of annual rate of increase. This pattern could be ascribed to the population dynamics and the peri-urban nature of the basin. This observation agrees with Ghana Statistical Service (2021), which reported that majority of the MDAs in the Upper West region are situated in the catchment of the basin. This was corroborated by the findings of Osman et al. (2025) in the KRB, which reported that eight out of eleven MDAs are located in the basin, which lends credence to the impacts of human activities in the basin. Furthermore, an increase in urbanization is generally associated with the expansion of infrastructure, resulting in the clearing of vegetation for construction purposes. This observation is supported by the findings of Tahiru et al.(2020) and Nasare et al. (2023) in the middle section basin of the WVB.

The light savannah forest in the basin continued to witness the highest expansion rate of 31.76% annually. The increase in grassland and bare lands resulting from human activities such as the expansion of croplands, settlements, bush burning, overgrazing, and bad farming practices may be accounting for this increased pattern. More significantly, the perennial bushfires in the basin pose a considerable threat to vegetation regrowth and contribute to the continuous loss of vegetation in the basin (Nasare et al., 2023; Aabeyir et al., 2024). This pattern aligns with the findings of Kumah et al. (2026), who reported an increase in built-up areas and grasslands, with a decline in closed savannah forest in the Nasia basin. Similarly, Nasare et al. (2023) corroborated this trend in the Nawauni catchment, where pervasive sand winning activities were identified as major contributors to the decline in vegetative cover and the shrinking of watercourses.

Also the distribution of dense savannah forest in the basin witnessed a consistent declining trend, with an average annual reduction rate of 13.90%. This negative trend may be linked to the expansion of built -up area and an increase in light savannah forest within the basin. This declining trend of dense savannah forest is likely to stem from unsustainable farming practices, illegal mining, and sand-winning activities in the basin. These findings agree with those of Nyadzi et al. (2021) in the Nasia basin, Nasare et al.(2023) in the Dallung catchment, and Aabeyir et al.(2024) in the Gbele forest reserve, all located within the WVB of Ghana.

Table 6. Distributions of LULC types of the KRB 1995-2023

LULC Class	Area (km^2)			
	1995	2005	2015	2023
Agricultural lands	905 (8.45%)	963(8.99%)	1008(9.44%)	1033(9.65%)
Built-up areas	2953(27.58%)	3140(29.33%)	3203.9(30%)	3400.9(31.79%)
Dense savannah forest	1792.5(16.74%)	1581.3(14.77%)	1241.9(11.63%)	1331.7(12.44%)
Light savannah forest	3211.4(29.99%)	3400.2(31.76%)	3480.2(32.59%)	3491.7(32.63%)
Water bodies	1843.3(17.22%)	1621.1(15.14%)	1745.5(16.34%)	1474.6(13.78%)

3.3 LULC transition rate in the KRB

The transition rate for built-up areas, agricultural lands, dense savannah forest, light savannah forest, and water bodies in the basin was assessed over the study period (Table 7). This highlights how various LULC types have been converted into other land types in the basin.

Table 7. Conversion matrix of LULC of KRB 1995-2023.

LULC Types	BLT	%	WTR	%	DF	%	LF	%	Agric	%
Built UP	891.24	8.33	0.03	2.34	1.12	0.01	413.63	3.84	415.17	3.81
Water bodies	377.98	3.53	1.34	0.01	8.35	0.08	234.62	2.2	2.3	0.02
Dense forest	2230.48	20.83	0.87	0.01	312.77	2.92	3033.12	28.34	345.32	3.22
Light forest	223.37	1.95	1.54	0.01	162.7	1.51	5087.39	47.53	83.47	0.78
Agricultural	668.96	6.25	81.32	0.76	100.13	0.94	298.46	2.79	68.76	0.64

Note. BLT= Built-up, WTR = Water, DF = Dense Forest, LF = Light Forest , Agric = Agricultural

From Table 7, built area witnessed a significant expansion of 8.33%, indicating the dominance of urbanization in the basin. It can be noted that 3.84% of light savannah forest and 3.81% (4.15km) of agricultural land have been converted into built-up areas, which demonstrated the peri-urban nature of the basin. This is associated with high population growth, in addition to high infrastructure development. Dense savannah forest experienced a significant reduction of 2.92%, remaining unchanged; 20.83% converted into built-up areas; 28.34% to light savannah forest; and 3.22% to agriculture. These findings revealed widespread deforestation, illegal mining activities, unsustainable commercial agricultural activities, and an urbanisation drive in the basin

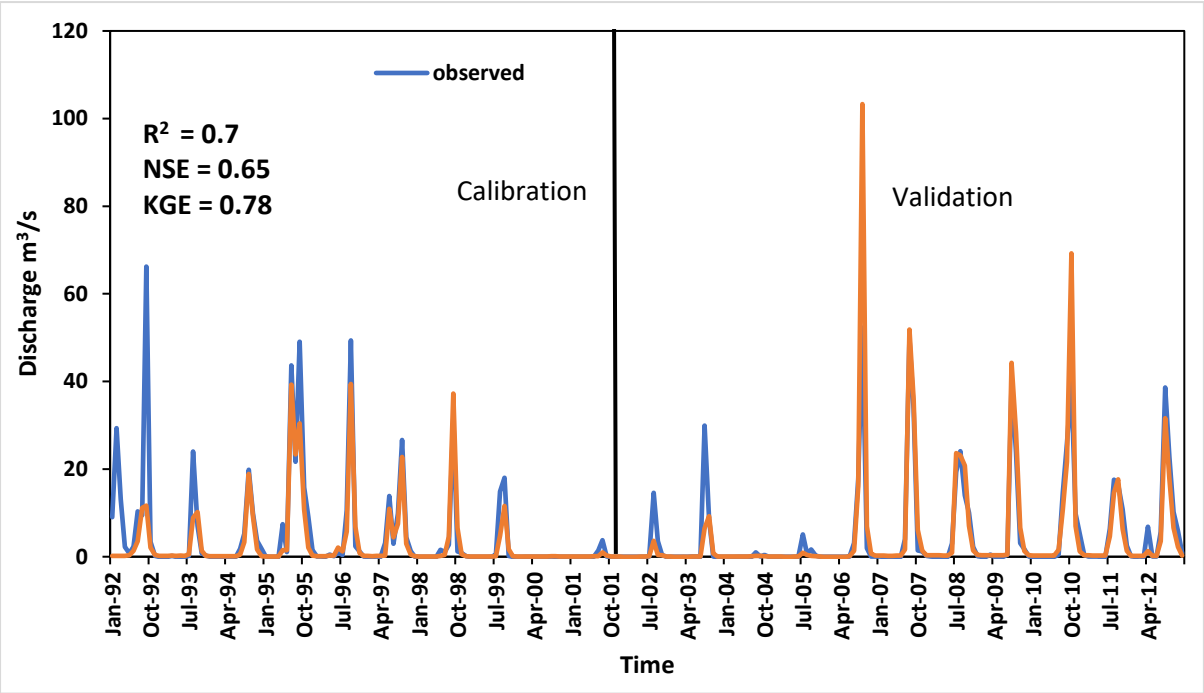
Light savannah vegetation was the dominant LULC type under the study period, and expanded by 47.53%, with a small portion converted into other land uses. About 1.95% of light savannah forest has transitioned into built-up areas, with 2.20% to water bodies, and 1.51% to dense forest. This increase in dense vegetation may be attributed to an ongoing afforestation project in the basin. Furthermore, the increased dominance of light vegetation in the basin is likely to be influenced by expansion in croplands, annual fires, illegal mining activities, and overgrazing. This suggests that the landscape in the basin is increasingly under anthropogenic pressure.

The transition matrix of the LULC in the basin reveals a rapidly evolving landscape, characterized by expansion of built-up areas at the expense of light savannah forest and agricultural land. There is a significant reduction of dense forest and water bodies, which highlights the potential threats to ecosystem services. Furthermore, the increase in light savannah forest could indicate a transition toward less dense or disturbed vegetative cover, which is largely driven by anthropogenic activities and land degradation processes.

3.4 Hydrological assessment of the KRB

3.4.1 Hydrological performance assessment of the SWAT model in the KRB

Results from the calibration and validation (Figure 6) demonstrated strong model performance**.** R^2 indicated that the model could explain about 70.0 % of the observed variance. The NSE showed that the model accounted for about 65% of the mean observed values, while the KGE revealed that the model could capture approximately 78.0 % of the variability in observed hydrological data. These results suggest that the SWAT model adequately simulated the flow dynamics of the KRB and can be used for further processing and analysis. This pattern aligned with studies by Mekonnen and Manderso (2023), who revealed that NSE performance of the SWAT runoff model could exceed 0.8 in small, humid watersheds; however, it generally remains below 0.7 in larger river basins. In this study, the model performance was considered adequate.



519

520 **Figure 6. Observed and simulated monthly water flow for the calibration and validation**
521 **periods.**

522 The evaluation of the simulated outputs showed good agreement with the average monthly
523 rainfall pattern of the basin (Figure 6). Despite this, a consistent trend of peak flow
524 underestimation was observed. Similar patterns have been reported by Kibii et al. (2021) in the
525 Kaptagat River catchment in Kenya and Lukas et al. (2025) in the Omo-Gibe River Basin in
526 Ethiopia. Furthermore, similar trends have also been reported by Mwanga et al. (2024) in the
527 Bontaga irrigation dam, Issahaku (2023) in the Tono irrigation dam, and Nyadzi et al. (2021)
528 in the Nasia sub-catchment of the White Volta basin. The key contributing factor to this
529 underestimation is the Curve Number (CN) method used in the SWAT model, which often fails
530 to adequately account for rainfall intensity. This limitation has also been identified by Tumsa
531 et al. (2022) and Kimbi et al. (2024) as a common phenomenon in hydrological modelling.

532 **3.5 Impacts of LULC on hydrological processes of the KRB**

533 The effects of LULC changes on the water balance components of the basin was assessed
534 (Table 8) using nine hydrological parameters simulated by the SWAT model; precipitation
535 (Precip), potential evapotranspiration (PET), evapotranspiration (ET), soil water content (SW),
536 percolation (PerC), surface runoff (SurfQ), groundwater flow (GWQ), water yield (WYLD),
537 and lateral flow (LatQ). The hydrological responses under four LULC scenarios, 1995, 2005,

2015, and 2023, were analyzed (Table 8) to illustrate the spatio-temporal variations in the basin's hydrological processes.

The results revealed a generally decreasing trend of precipitation from 2691 mm to 2633.25 mm (2.14%) over the study period in the basin and an increase in temperature. This pattern may be attributed to the loss of vegetation cover, largely due to high anthropogenic activities in the basin (Nyadzi et al., 2021). This observation is consistent with the findings of Abungba et al.(2022), Malede et al.(2023), and Arthur et al.(2025), who reported similar trends in the Black Volta, the Abbay Basin in Ethiopia, and the Pra Basins in Ghana.

PET remained relatively constant (5140.85mm) over the study period, with a net value of -0.075 mm, which represents (-0.0015%), indicating a negligible long-term variation. These observations may be linked to variations in temperature and other climatic drivers, which point to the influence of climate variability rather than LULC changes. However, while LULC changes may not directly affect PET significantly, compared to other hydrological parameters, some anthropogenic activities in the basin, such as annual burning, land clearing, and increased water abstraction, may contribute to altering local microclimatic conditions in the basin. These practices could modify the heat fluxes and atmospheric moisture content, which can influence localized PET patterns over time. Despite this, the changes in net values of PET suggest that land use activities might have significantly altered the PET pattern in the basin. This observation aligned with the findings of Malede et al. (2023), who also observed a similar pattern and attributed this to the high anthropogenic activities.

ET declined by 4.91%, from 1811.63 mm to 1722.78 mm. This trend may be attributed to the reduced vegetation cover resulting from the conversion of dense savannah forest to light savannah forest (Tables 6 and 7). These transitions are strongly driven by expansion in croplands, increase in built-up areas, urbanization, illegal gold mining activities, deforestation, and expansion of agricultural lands. These observations are consistent with the findings of Osman et al. (2025), Nasare et al.(2023), and Tengapoe et al.(2023) in the White and Black Volta Basins of Ghana. These practices result in the removal of natural vegetation, which plays a critical role in facilitating water loss through transpiration and evaporation. As vegetative cover diminishes, the capacity of the land to return water to the atmosphere through ET decreases, leading to lower ET values. These findings align with studies by Tola and Deyassa, (2024) in the Walga and Upper Omo Basin of Central Ethiopia, Abuhay et al. (2023) in the Upper Gilgil Abbay Watershed of Ethiopia, and Umukiza et al. (2024) in the dam catchments

of northern Ghana. These studies established a positive correlation between ET and vegetative cover and concluded that the decline in ET in the study areas was attributed to the significant vegetative cover loss, largely due to the expansion of cultivated land and built-up areas. This may not only alter the hydrological balance of the basin but may have broader implications for local microclimates, soil moisture retention, and ecosystem health.

SurfQ shows an increasing trend of 7.78% and a decline of PerC by 4.87%. The increase in SurfQ in the basin could be linked to the loss of vegetative cover caused by the expansion of built-up areas. These activities reduced the infiltration rate, leading to high overland flow, which may result in elevated soil erosion, flash floods, and sediment loads in the basin. These findings align with the conclusions of Abungba et al. (2022) in the Black Volta basin, Umukiza et al. (2024) on the dam catchment of northern Ghana, and Aredehey et al. (2020) who reported that SurfQ in the Giba watershed of Ethiopia was largely influenced by the level of the vegetative cover index on the land surface.

GWQ showed a net increase of 4.14%, despite some variability; groundwater contribution remained relatively stable, indicating modest changes in subsurface dynamics, despite reduced percolation. WYLD witnessed a significant decline of 14.5%, which signifies an overall decline in water resources in the basin. This reduction may be attributed to a decrease in precip, infiltration, and ET as a result of an increase in anthropogenic activities. According to Osman et al.(2025), the KRB is undergoing rapid urbanization, with about 85.0% of the MDAs located in the basin. The high population growth and infrastructure expansion have increased water demand, potentially threatening GWQ levels due to intensified groundwater abstraction. This pattern aligns with the findings of Hyandye et al. (2018), who associated the decline in GWQ in the Ndembera watershed of Tanzania with deforestation and high water abstraction, and concluded that a decrease in GWQ is directly proportional to a decrease in vegetative cover. Ankomah et al. (2021) also indicated that GWQ in the Densu Basin of Ghana is mostly influenced by forest cover and other LULC changes.

LATQ exhibited variability across the study period, with a slight overall decline of −1.87%. Although LATQ remained relatively stable, it remains sensitive to variations in land use and soil moisture conditions. The results suggested that LULC changes have a potential impact on soil infiltration and water storage capacity, which affects hydrological components of the basin. There was a strong relationship between LULC and hydrological components as well as climate

601 variables. These observations align with similar findings of Dibaba et al.(2020) and Mekonnen
602 and Manderso (2023).
603

604 **Table 8. Annual mean of hydrological variables of the KRB**

Hydrological variables	LULC Scenario				Rate of Change							
	1995 (mm)	2005 (mm)	2015 (mm)	2023 (mm)	1995-2005 (mm)	%	2005-2015 (mm)	%	2015-2023 (mm)	%	1995-2023 (mm)	%
PRECIP	2691	2653.17	2647.92	2633.25	-37.83	-1.41	-5.25	-0.19	-14.67	-0.55	-57.75	-2.14
PET	5140.85	5138.22	4974.47	5140.78	-2.63	-0.051	-163.75	-3.19	166.31	3.34	-0.075	-0.0015
ET	1811.63	1765.43	1724.71	1722.78	-46.20	-2.55	-40.72	-2.31	-1.93	-0.11	-88.854	-4.91
SW	1586.39	1739.38	1883.19	1709.86	152.99	9.64	143.81	8.27	-173.33	-9.206	123.47	7.78
PERC	1023.58	1017.57	998.71	973.69	-6.01	-0.58	-18.86	-1.85	-25.02	-2.51	-49.89	-4.87
SurfQ	6.622	7.35	8.56	9.99	0.728	10.99	1.21	16.46	1.43	16.71	3.368	50.86
GWQ	45.61	43.54	48.11	47.5	-2.07	-4.53	4.57	10.49	-0.61	-1.27	1.89	4.14
WYLD	70.39	68.14	64.62	60.18	-2.24	-3.19	-3.52	-5.17	-4.44	-6.87	-10.21	-14.50
LATQ	26.44	24.79	23.82	25.94	-1.64	-6.22	-0.97	-3.91	2.12	8.90	-0.49	-1.87

605

606

607

608

609

3.5.1 Impacts of LULC on seasonal and monthly variations in hydrological variables in the KRB

The seasonal variations of LULC on hydrologic variables in the basin were assessed (Figure 7) under two rainfall regimes, wet season (May to October) and dry season (November to April). The impact of LULC change was largely visible in the wet season compared to the dry season. This observation suggests that LULC changes have a strong influence on PET; for instance, PET exhibited seasonal variation, with the dry season accounting for 65-70% compared to the wet season 30–35% annually. On a monthly scale, the dry season recorded 10-12%, while the wet season recorded 4-6 %. Also, PET exhibited a marginal increase of 2-5% between 1995 and 2023, and a pronounced rise during the dry season, demonstrating the influence of LULC on atmospheric water demand.

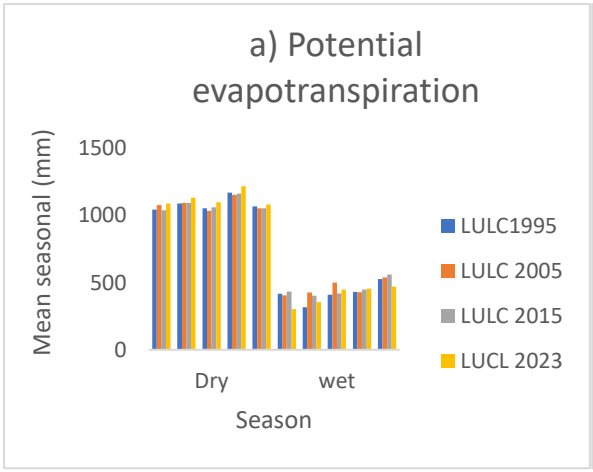
Precipitation in the dry season accounts for 20.0%, which creates significant water deficits in the basin and typically results in water scarcity. On a monthly scale, the dry season contributes 2.0-4.0% rainfall, whereas the wet season records 10.0-15.0% rainfall. This observation highlights a pronounced seasonal imbalance, where water stress prevails in the dry season and water abundance in the wet season. These findings are consistent with the results of Ampofo et al. (2020) in the Tono irrigation dam.

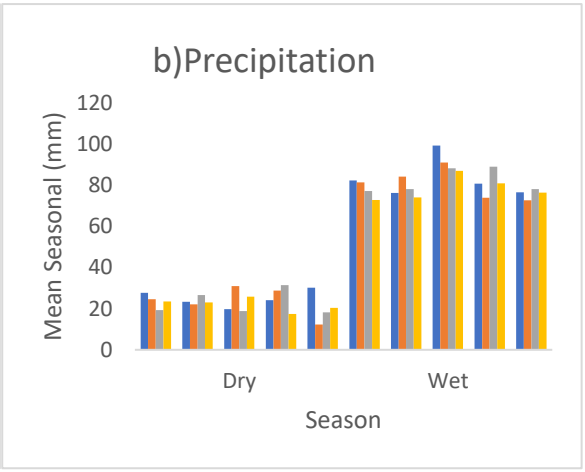
The ET was also more pronounced in the wet season, accounting for 70.00%-80.00% of the total annual ET, with 20.00-25.00% in the dry season. This indicates that ET is strongly controlled by rainfall availability and soil moisture recharge during the rainy season. The ET contribution in the dry season was much lower compared to the wet season. This observation may be ascribed to the fact that during the wet season, there is substantial vegetative cover compared to the dry season, therefore enhancing ET through transpiration and evaporation from moist soils.

Also, because the basin is agrarian in nature, large portions of the land are under rainfed cultivation. Croplands actively transpire when rainfall and soil moisture are abundant, which contributes significantly to the high values of ET recorded in the wet season. The lower ET values observed in the dry season could be linked to reduced biomass as croplands lie fallow, grasses dry out and burn, and degraded lands provide little vegetative cover. Forests and water bodies are the factors on land cover that help sustain ET during the dry season, but ongoing LULC changes have diminished this buffering capacity (Gashaw et al., 2018).

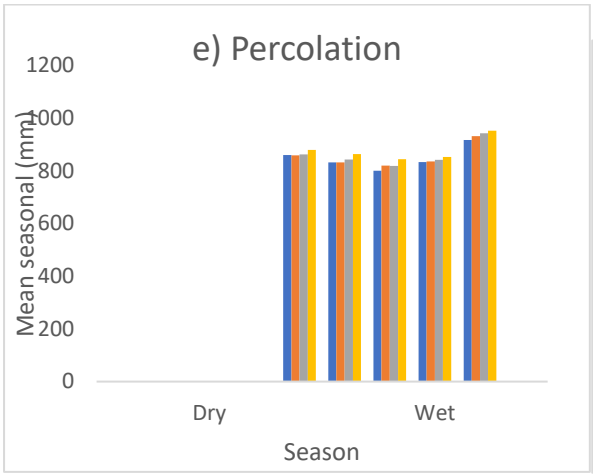
These seasonal variations highlight the influence of rainfall, vegetation cover, and soil moisture dynamics on ET. These findings agree with the results of Tola and Deyassa (2024), who observed a similar trend and concluded that low ET in the dry season was attributed to decreased forest cover. SurfQ in the basin was predominantly high in the wet season at 97.0%, with a little contribution of 2.0%, in the dry season. These seasonal variations, caused by rainfall and LULC variability, demonstrate the water scarcity challenges usually experienced during the dry season. The pattern may be due to an increase in croplands, resulting in reduced vegetative cover and poor vegetation interception. Addition to expansion of settlement patterns and bare lands increases impervious surfaces, reducing infiltration and enhancing flashy runoff during rainfall events. This finding is consistent with the results of Malede et al. (2023) in the Abbay Basin and Galata et al.(2020) in the Hangar watershed in Ethiopia, which concluded that the increase in SurfQ is influenced by LULC changes.

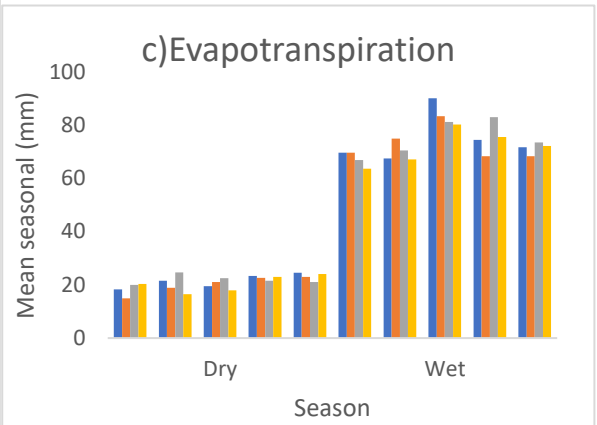
The results (Figure 7) also show that 80.0-90.0% of GWQ in the basin occurs in the wet season, while 10.0-20.0% occurs in the dry season, underscoring the dependence of GWQ on precipitation, soil water storage, and land cover dynamics. Cropland expansion, deforestation, and settlement growth have altered infiltration patterns, intensified wet-season recharge variability, and reduced the basin's resilience to sustain groundwater supplies in the dry season. Also, cropland expansion, deforestation, and wetland conversion have intensified wet-season recharge variability while reducing the capacity of the landscape to sustain groundwater contributions into the dry season. Furthermore, abundant rainfall in the wet season replenishes soil water and drives deep percolation, which enhances groundwater recharge. The relatively uniform high values recorded suggest that recharge is consistently strong across different LULC classes during the study period.



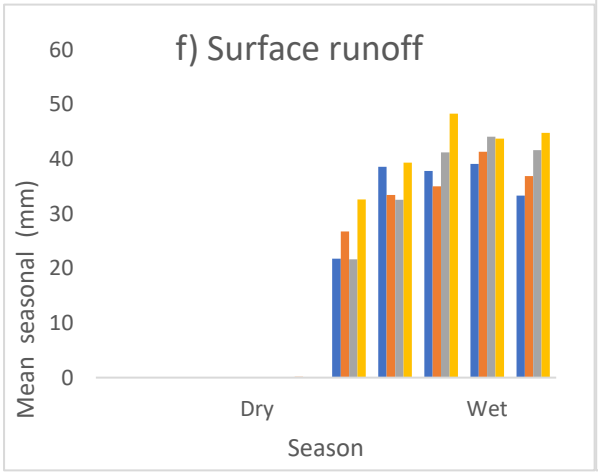


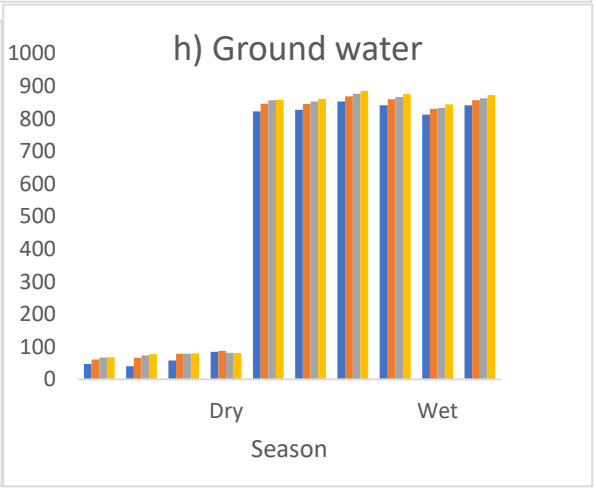
666





667





668

669

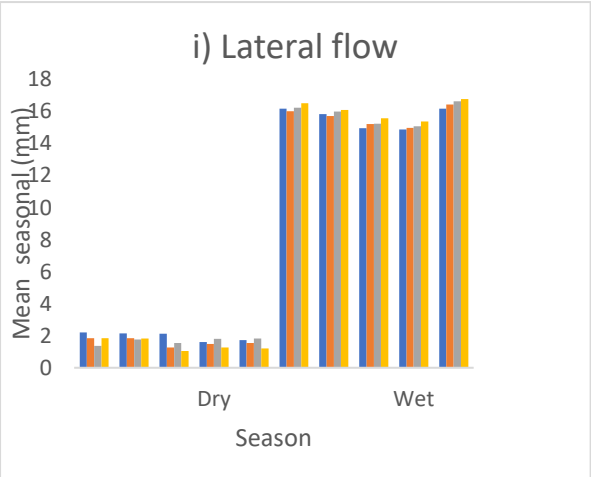


Figure 7: Mean Seasonal variation for PET, ET, Precip, PERC, SURQ, SW, GW, LATQ, WYD in the KRB from 1995 to 2023.

Figure 7 shows that high percolation rates were high in the wet season (90.0%) compared to the dry season (1.0%), indicating that percolation is strongly influenced by rainfall input and soil moisture recharge. In the wet season, intense and sustained rainfall drives infiltration beyond the root zone, leading to higher percolation. This directly supports GWQ, explaining why more than 80.0% of GWQ occurs during this period.

Despite the fact that rainfall is limited in the dry season, residual soil moisture and contributions from shallow aquifers sustain some level of percolation. These observations could be linked to the fact that in the wet season, there is abundant canopy cover from forests and woodlands, which promotes higher infiltration and percolation through the canopy cover and deep-rooting systems. These observations could be linked to the fact that in the wet season, there is abundant canopy cover from forests and woodlands, which promotes higher infiltration and percolation through the canopy cover and deep-rooting systems, while in the dry season, croplands and bare lands exhibit reduced infiltration due to soil compaction, exposure, and limited percolation in degraded areas.

Furthermore, LULC changes such as cropland expansion, deforestation, and expansion of built-up areas could significantly alter infiltration and percolation dynamics, reducing the basin's ability to buffer against dry season water scarcity, which intensifies the seasonal variations in water availability. These findings agree with the works of Gashaw et al.(2018), who attributed the increase in GWQ to an increase in agricultural activities and settlement patterns.

The analysis of LATQ in the basin exhibited a seasonal trend, with the wet season accounting for about 70.0-80.0% and 20-30% for the dry season. These strong variations may be

694 influenced by LULC. Forested areas enhance infiltration and maintain LATQ even after rainfall
695 events, while cropland and built-up areas may reduce subsurface storage, leading to a marked
696 decline in LATQ in the dry season. The transition of LULC from savannah forest to cropland
697 intensified surface runoff at the expense of LATQ, increasing streamflow in the wet season and
698 reducing baseflow during the dry season. Also, an increase in agricultural activities and
699 deforestation reduces soil porosity and infiltration, decreasing lateral flow. This observation
700 agrees with the findings of Nigusie and Dananto (2021), who reported an increase in the LATQ
701 in the wet season compared to the dry season as a result of the dynamics of LULC. Built-up
702 areas also increase impervious surfaces, almost diminishing the contributions of subsurface
703 flow, and worsening water scarcity in the dry season.

704 **3.6 Impact of LULC change on hydrological variables at the sub-basin level of the KRB**

705 The mean relative percentage change in Precip, PET, ET, WYLD, GWQ, SurfQ, and LATQ
706 were analyzed at the sub-basin level (Figure 8). Precip across the basin exhibited a general
707 decreasing trend, with the middle and southern parts showing a modest increase of 5.28-5.42%.
708 This decline can be attributed to LULC changes, particularly in the northern sections of the
709 basin, where extensive deforestation, agricultural expansion, illegal mining activities, and
710 annual bushfires significantly reduced natural vegetation cover. This affects ET and
711 atmospheric moisture, resulting in reduced precipitation. The middle and southern portions of
712 the basin exhibited a different trend, which could be linked to the relative abundant vegetation
713 cover and forests, especially those within the Gbele park in the basin. These areas provide more
714 favourable microclimatic conditions that enhance ET and localized convection, supporting
715 rainfall. This spatial pattern is consistent with findings by Achugbu et al. (2022) and Ngondo
716 et al. (2022), who observed that LULC transitions strongly influence spatial variations in
717 hydrological processes and rainfall distribution.

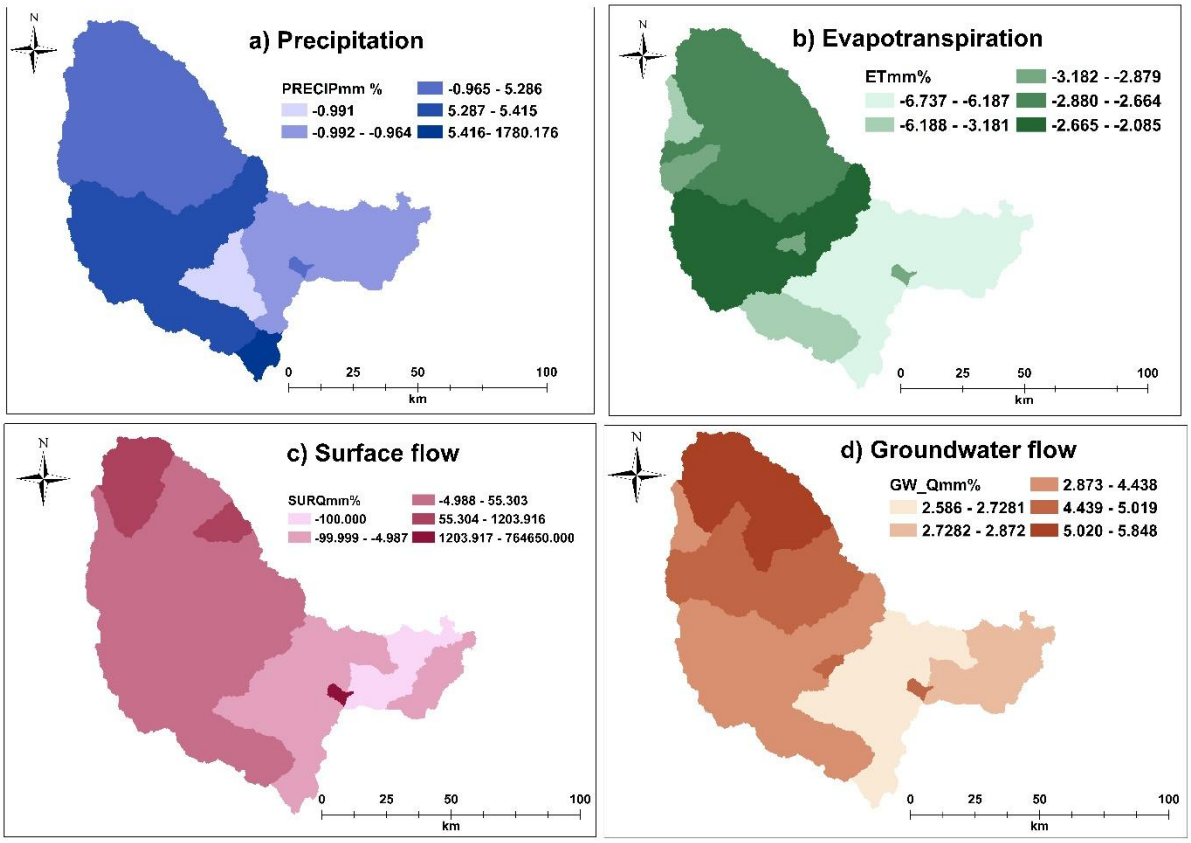
718 ET exhibited a decreasing trend of 2.09-6.74% in the basin, which can be strongly linked to
719 widespread deforestation, expansion of settlements, and croplands, which have reduced
720 vegetative cover. This limits canopy interception, transpiration, and soil moisture retention.
721 These changes decrease overall ET rates. Similarly, the conversion of natural vegetation into
722 farmlands exposes soils, leading to faster drying and reduced ET rates. This trend aligns with
723 the observations of Achugbu et al. (2022), who noted that LULC changes, such as deforestation
724 and agricultural expansion, have a pronounced impact on ET, with the strongest reductions
725 occurring in areas of intensive land degradation. Also, Nsiah et al.(2021) reported similar

findings in the Pra Basin and concluded that LULC changes have a strong influence on ET, and the rate could vary depending on the LULC types.

SurQ largely increased across the basin, with a slight decrease in the south-easternmost part of the basin. This increase in SurQ could be due to the LULC changes, particularly the conversion of dense savannah into croplands, built-up areas, and light savannah forest, which have reduced vegetation cover, decreased infiltration, and made the soils more compacted and exposed. This pattern demonstrates how changes in LULC types directly alter the hydrological balance of the basin, with vegetation loss driving higher runoff generation, while areas with residual cover and regulated land use show moderated responses. This is consistent with the findings of Ampofo et al.(2022), who reported similar results and attributed these changes to human activities such as Agriculture.

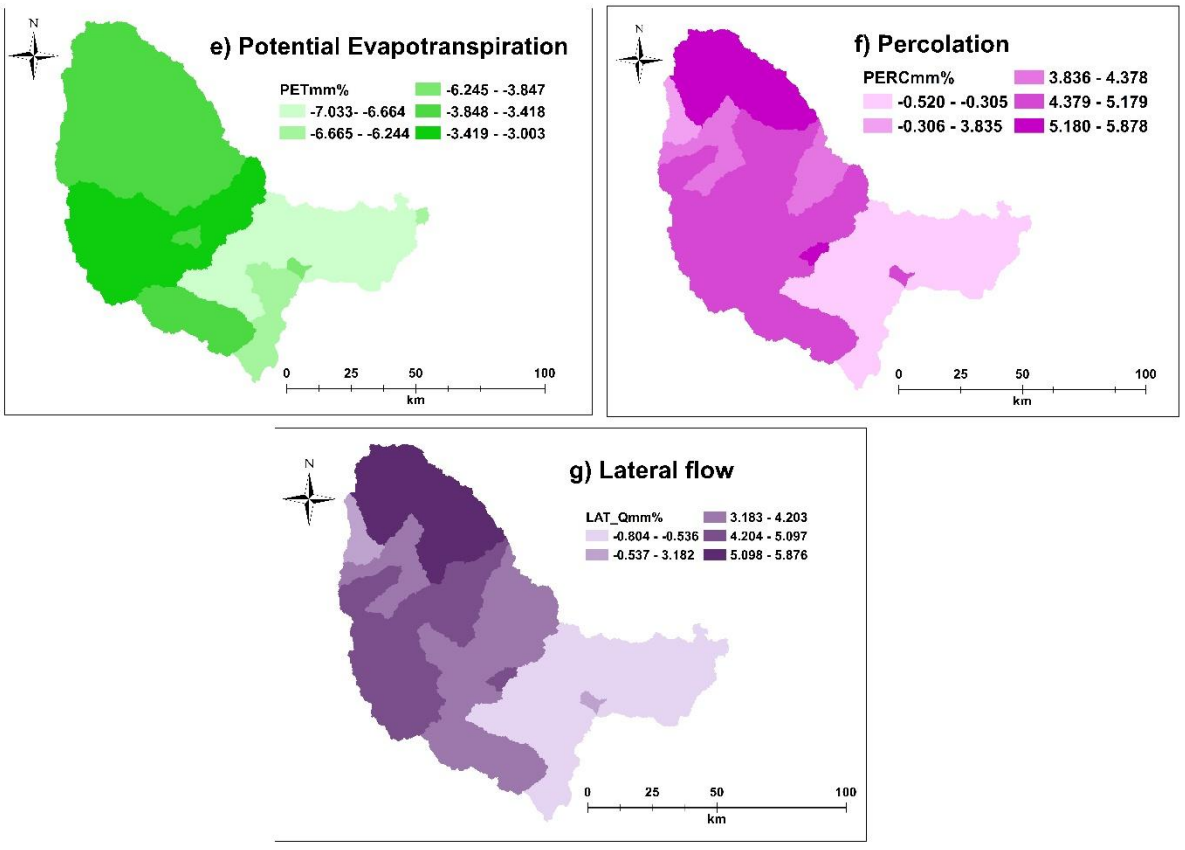
PET exhibited a decreasing trend with a pattern closely linked to LULC changes across the basin. The transition from dense vegetation to croplands and bare lands decreases vegetative cover and the atmospheric demand for water, further reducing the PET rate. Also, built-up areas and degraded lands contribute to this decline. Impervious surfaces limit soil moisture availability for evaporation, while degraded soils in farming zones lose their organic content and capacity to hold water, reducing evaporation from the soil surface. This finding contradicts that of Nyadzi et al. (2021) in the Nasia sub-basin of the WVB, where they attributed an increase in PET to increased wind speed and rising temperature.

The general increase in LATQ also reflects the effects of land degradation, bushfires, and deforestation, which expose soils, reducing organic matter content and weakening soil structure. Under such conditions, infiltration still occurs but tends to favour shallow subsurface pathways rather than vertical percolation, thereby increasing lateral contributions to streamflow.



751

752



753

754 **Figure 8: Sub-basin level percentage changes in some key hydrological variables**

3.7 Impacts of LULC on hydro-climatic variables

3.7.1 Effects of LULC on rainfall and temperature variability in the KRB.

The effects of LULC changes on temperature and precipitation were analyzed to determine their implications for the water balance components of the KRB (Figure 9), under two emission scenarios (SSP1-2.6 and SSP5-8.5). The results revealed that LULC has a strong positive correlation with both temperature and precipitation in the basin, suggesting that changes in land cover significantly influence hydro-climatic variables. The results further demonstrated that an increase in temperature under both scenarios corresponded with a decrease in precipitation. From 1995 to 2023 (Table 7), temperature increased by 12.48%, and precipitation decreased by 3.47% under the SSP5-8.5 scenario. This indicates a considerable rate of change in both variables, with serious implications for hydrological processes and water balance components in the basin.

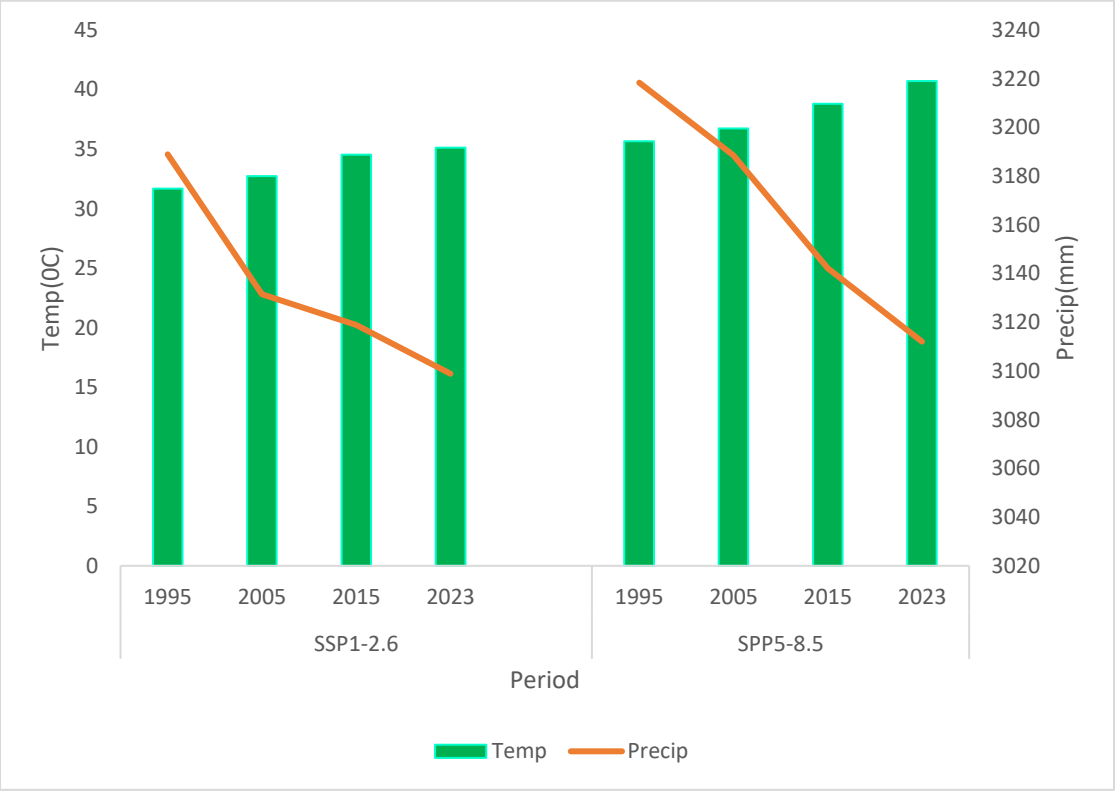


Figure 9. Trend of LULC on temperature and Precipitation in the KRB from 1995 to 2023

Largely, the effects of climate change on the KRB can be understood through the combined influence of precipitation, temperature, and evapotranspiration. Reduction in rainfall diminishes the amount of water contributing to surface runoff, while rising temperatures intensify evapotranspiration losses. These processes decrease overall water availability in the basin, which accounts for the observed reduction in runoff. This has resulted in a decrease in

WYLD by 14.50%, ET by 4.90%, LatQ 1.80%, and PERC 4.87%. These findings highlight the combined effects of LULC changes and climate variability on the water balance components of the basin, with implications for streamflow, groundwater recharge, and ecosystem services.

The changes in the hydrologic processes of the basin can largely be attributed to the decline in vegetation cover, driven by the conversion of dense savannah vegetation into light savannah, croplands, and built-up areas. Vegetation plays a critical role in regulating hydrological processes by enhancing infiltration, promoting percolation, and sustaining evapotranspiration (Malede et al., 2023). When vegetation is reduced, infiltration capacity declines, leading to lower percolation rates and reduced groundwater recharge (Kibii et al., 2021). Similarly, ET decreases due to reduced canopy cover and diminished root-water uptake.

As a result, these land cover changes alter the water balance components of the basin. Less infiltration and groundwater recharge increase the proportion of rainfall that is converted into surface runoff, while reduced ET and vegetation cover weaken the natural buffering capacity of the ecosystem. This translates into lower precipitation recycling, greater surface runoff, and diminished groundwater storage, thereby intensifying the hydrological impacts of climate change in the basin. These findings are consistent with those of Kibii et al.(2021), who reported similar hydrological responses in the Kaptagat Basin in Kenya. Furthermore, Frimpong et al. (2022) also observed that LULC changes have contributed to rising temperatures and precipitation, which contradicts the findings of this study, where precipitation exhibited a decreasing trend

3.8 Rate of change of temperature and precipitation in the KRB

The mean annual rate of change of temperature and precipitation in the KRB was assessed (Table 9) under two emission scenarios (SSP1-2.6 and SSP5-8.5) for the period 1995-2023. Results indicate that under SSP5-8.5, temperature exhibited a significant increasing trend compared to SSP1-2.6 between 1995 and 2023. The result revealed further that temperature increased by 50.00%, with a rate of change of 12.48%, with the most pronounced increase occurring between 2005 and 2015. These findings suggest that under SSP5-8.5, both maximum temperature (Tmax) and minimum temperature (Tmin) increased at a faster rate than under SSP1-2.6, indicating the severe warming effects of high emissions.

Precipitation under SSP5-8.5 also showed a significant declining trend compared to SSP1-2.6. The largest reduction occurred in 2005-2015. Cumulatively, rainfall decreased by 50.0% from 1995 to 2023 at a rate of 3.42%. This implies that the high-emission scenario intensifies rainfall

decline, with cascading effects on water scarcity, groundwater recharge, and streamflow in the basin.

From this pattern, it can therefore be concluded that Tmax and Tmin increased under both SSP1-2.6 and SSP5-8.5; however, the warming effects were more pronounced under SSP5-8.5. This points to stronger nighttime warming under high-emission conditions. Similarly, precipitation witnessed a declining trend under both scenarios, with a greater reduction observed under SSP5-8.5. The combined effect of increasing temperature patterns and declining rainfall regimes explains the observed reductions in runoff, groundwater recharge, and overall water yield in the KRB. This has serious ramifications for the water balance component of the basin, with cascading effects on agriculture and ecosystem sustainability.

820

821 **Table 9. Mean annual rate of change of temperature and Precipitation in the Kulpawn basin**

Scenarios		Changes				Rate of change (%)			
	Temp(^{0}C)	1995-2005	2005-2015	2015-2023	1995-2023	1995-2005	2005-2015	2015-2023	1995-2023
SSP126	Tmax	1.04(20.97%)	1.8(36.26%)	1.02(20.46%)	1.11(22.30%)	3.29	5.51	2.95	3.16
	Tmin	0.5895(-6.55)	0.28(20.30)	0.5(36.25)	0.689(50.00)	-0.41	1.26	2.23	3.07
SSP585	Tmax	1.09(10.81)	2.07(20.33)	1.92(18.85)	5.08(50.00)	3.08	5.63	4.94	12.48
	Tmin	1.56914.77)	1.47(13.92)	2.25(21.32)	5.29(49.85)	7.19	6.32	9.11	19.58
SSP126	Precip(mm)	-57.5(31.92)	-12.56(6.97)	-20.1(11.10)	-90.06(49.56)	-1.803	-0.401	-0.64	-2.91
SSP585	Preicip	-29.77(0.144)	-46.52(0.219	-30.05(0.141)	-106.34(50.00)	-0.924	-1.46	-0.96	-3.417

822

4.0 Conclusions

LULC changes driven by agricultural expansion, urbanization, deforestation, illegal mining, and fuelwood extraction have caused significant modifications of the KRB from 1995 to 2023. Agricultural land and built-up areas expanded significantly, while dense savannah forest and water bodies declined. The expansion of built-up areas by 20.83% and the widespread conversion of dense vegetation into agricultural and light savannah forest by 47.53% signify the intensity of the anthropogenic footprint on the basin hydrology.

The results revealed that temperature increased by 12.48%, and precipitation declined by 3.47% under SSP5-8.5 scenario, indicating a pronounced warming and drying trend across the basin. The strong correlation between LULC changes and hydro-climatic variables suggests that alterations in land cover significantly influence local rainfall and temperature dynamics in the basin. These transformations have disrupted the hydrological balance of the basin, leading to decreased infiltration and groundwater recharge, increased surface runoff, and reduced evapotranspiration. The combined effects have resulted in more frequent wet-season flooding and heightened dry season water scarcity patterns that are expected to intensify.

These findings highlight the pressing need to implement sustainable land management practices, such as reforestation programs and integrated watershed management approaches, to mitigate the adverse impacts of LULC and climate change. Strengthening vegetation cover through afforestation and sustainable agricultural practices can enhance infiltration, stabilize runoff, and restore the natural hydrological regulation of the basin. Implementing these adaptive measures is crucial for improving ecosystem resilience, water resources, and promoting long term hydrological and environmental sustainability within the KRB.

4.1 Policy and management implications

The observed LULC changes and their impacts on the hydrological balance of the KRB highlight the urgent need for coordinated policy interventions and adaptive management strategies. The following policy and management measures are recommended to promote sustainable land and water resource management in the basin.

- Implement and enforce spatial land use plans at both district and watershed levels. Integrate land use and hydrological data into local and regional planning to ensure

balanced development, reduce environmental degradation, and prevent the encroachment of human settlements into sensitive ecological zones.

- ❖ Conversion of dense vegetation into agricultural land reflects unsustainable farming practices that contribute to soil degradation and reduced water retention. To address this, policies should promote climate-smart and conservation agriculture to conserve soil moisture and reduce erosion.
- ❖ The adoption of agroforestry systems, cover cropping, and minimum tillage should be encouraged, with the provision of incentives for farmers who practice sustainable land management techniques.
- ❖ Prioritization of community-based reforestation and afforestation programs using native species to restore degraded lands and enhance natural hydrological regulation.
- ❖ Interventions such as rainwater harvesting, construction of small-scale reservoirs, and soil-water conservation structures can support water security, while improved monitoring of surface and groundwater resources will ensure their sustainable use and equitable allocation.
- ❖ Establish basin-level stakeholder platforms involving the Environmental Protection Authority (EPA), Water Resources Commission, Forestry Commission, local assemblies, and community groups to foster collaboration and shared responsibility.
- ❖ Build the capacity of local communities through participatory land and water governance frameworks to enhance ownership and ensure the long-term success of conservation initiatives.
- ❖ Establish long term monitoring systems using remote sensing, GIS, and hydrological models to facilitate the tracking of LULC changes, climate variability, and hydrological responses.

Funding

This work has been produced with the financial assistance of the European Union (Contract number: AFS2023/444-387). The contents of this document are the sole responsibility of the authors and can under no circumstances be regarded as reflecting the position of the European Union.

Data Availability statement

Data is available upon request from the corresponding author.

Author statement

Z.O: Wrote the full manuscript text, conceptualization, Methodology, Investigation, and data curation. **C. G:** Manuscript writing, software, supervision, reviewing, and editing. **B. E**: Supervision, visualization, reviewing, and editing. **O.S.A**: Validation, supervision, reviewing, and editing. **G.K.A**: Reviewing and editing. **K.M:** Software, validation, and preparation of figures. **O.A.K.A:** Validation and preparation of figures

Declaration

The authors declare no competing financial or personal interests.

Ethics approval and consent to participate

Not applicable. This study does not involve human subjects, animals, or any sensitive data.

Consent for publication

Not applicable

Acknowledgment

The first author acknowledges the partial financial support received from the Ghana Education Trust Fund (GETFund). In-kind contributions from the Regional Water and Environmental Sanitation Centre, Kumasi (RWESCK), at the Kwame Nkrumah University of Science and Technology (KNUST), Kumasi, for the doctoral studies are also deeply appreciated.

References

Aabeyir, R., Peprah, K., and Amponsah, A. (2024). Temporal analysis of the state of the Gbele Resource Reserve in the Upper West Region, Ghana. *Frontiers in Forests and Global Change*, *7*(March), 1–9. https://doi.org/10.3389/ffgc.2024.1353852

Abuhay, W., Gashaw, T., and Tsegaye, L. (2023). Assessing impacts of land use/land cover changes on the hydrology of Upper Gilgel Abbay watershed using the SWAT model. *Journal of Agriculture and Food Research*, *12*, 1–38. https://doi.org/10.1016/j.jafr.2023.100535

Abungba, J. A., Adjei, K. A., Gyamfi, C., Odai, S. N., Pingale, S. M., and Khare, D. (2022). Implications of Land Use/Land Cover Changes and Climate Change on Black Volta Basin Future Water Resources in Ghana. *Sustainability (Switzerland)*, *14*(19). https://doi.org/10.3390/su141912383

916 Achugbu, I. C., Olufayo, A. A., Balogun, I. A., Dudhia, J., McAllister, M., Adefisan, E. A., and
917 Naabil, E. (2022). Potential effects of Land Use Land Cover Change on streamflow over
918 the Sokoto Rima River Basin. *Heliyon*, *8*(7).
919 https://doi.org/10.1016/j.heliyon.2022.e09779

920 Adzawla, W., Azumah, S. B., Anani, P. Y., and Donkoh, S. A. (2020). Analysis of farm
921 households' perceived climate change impacts, vulnerability and resilience in Ghana.
922 *Scientific African*, *8*. https://doi.org/10.1016/j.sciaf.2020.e00397

923 Aladejana, O. O., Salami, A. T., and Adetoro, O. I. O. (2018). Hydrological responses to land
924 degradation in the Northwest Benin Owena River Basin, Nigeria. *Journal of*
925 *Environmental Management*, *225*(July), 300–312.
926 https://doi.org/10.1016/j.jenvman.2018.07.095

927 Amini, S., Saber, M., Rabiei-Dastjerdi, H., and Homayouni, S. (2022). Urban Land Use and
928 Land Cover Change Analysis Using Random Forest Classification of Landsat Time Series.
929 *Remote Sensing*, *14*(11), 1–23. https://doi.org/10.3390/rs14112654

930 Ampofo, S., Ampadu, B., Douti, N. B., and Kusibu, M. M. (2020). Modeling soil water balance
931 of an agricultural watershed in the Guinea Savannah Agro-ecological Zone; a case of the
932 Tono irrigation dam watershed. *Ghana Journal of Science, Technology and Development*,
933 *7*(1), 69–81. https://doi.org/10.47881/223.967x

934 Ampofo, S., Boadi Manu, M. A., Ampadu, B., and Adonadaga, M.-G. (2022). Impact of
935 Landuse and Landcover Changes on Hydrological Components of the Oti Sub-Basin of
936 Ghana. *Ghana Journal of Science, Technology and Development*, *8*(2), 60–70.
937 https://doi.org/10.47881/375.967x

938 Ankomah-Baffoe, J., Yawson, D. O., and Okae-Anti, D. (2021). Assessment of the Impacts of
939 Climate Change on Some Hydrological Processes of The Densu River Basin, Ghana.
940 *Ghana Journal of Geography*, *13*(1), 147–166. https://doi.org/10.4314/gjg.v13i1.8

941 Aragaw, H. M., Mishra, S. K., and Goel, M. K. (2022). Responses of water balance
942 components to land use/land cover and climate change using geospatial and hydrologic
943 modeling in the Gidabo watershed, Ethiopia. *Geocarto International*, *37*(27), 17119–
944 17144. https://doi.org/10.1080/10106049.2022.2123956

945 Arfasa, G. F., Owusu-Sekyere, E., and Doke, D. A. (2024). Climate Change Projections and
946 Impacts on Future Temperature, Precipitation, and Streamflow in the Vea Catchment,
947 Ghana. *Environmental Challenges*, *14*(December 2023), 100813.
948 https://doi.org/10.1016/j.envc.2023.100813

949 Arifeen, H. M., Phoungthong, K., Mostafaeipour, A., Yuangyai, N., Yuangyai, C., Techato, K.,
950 and Jutidamrongphan, W. (2021). Determine the land-use land-cover changes, urban
951 expansion and their driving factors for sustainable development in Gazipur Bangladesh.
952 *Atmosphere*, *12*(10). https://doi.org/10.3390/atmos12101353

953 Arthur, E., Gyamfi, C., Kyekyeku Anyemedu, F. O., and Gyampo, M. (2025). SPATIAL and
954 temporal dynamics of groundwater vulnerability to contaminants under climate and land
955 use changes in the Pra and Ankobra basins. *Watershed Ecology and the Environment*,
956 *7*(May), 208–229. https://doi.org/10.1016/j.wsee.2025.05.001

957 Asante-Yeboah, E., Ashiagbor, G., Asubonteng, K., Sieber, S., Mensah, J. C., and Fürst, C.
958 (2022). Analyzing Variations in Size and Intensities in Land Use Dynamics for Sustainable
959 Land Use Management: A Case of the Coastal Landscapes of South-Western Ghana. *Land*,

11(6), 1–28. https://doi.org/10.3390/land11060815

Azumah, S. B., Adzawla, W., Donkoh, S. A., and Anani, P. Y. (2021). Effects of climate adaptation on households' livelihood vulnerability in South Tongu and Zabzugu districts of Ghana. *Climate and Development*, *13*(3), 256–267. https://doi.org/10.1080/17565529.2020.1757398

Baffour-Ata, F., Antwi-Agyei, P., and Nkiaka, E. (2021). Climate variability, land cover changes and livelihoods of communities on the fringes of Bobiri Forest Reserve, Ghana. *Forests*, *12*(3), 1–24. https://doi.org/10.3390/f12030278

Baral, K., Pandey, V. P., Pradhan, A. M. S., and Khanal, A. (2023). Impacts of Climate Change and Land Use Change on Streamflow: A Case of Seti Gandaki Watershed, Nepal. *Journal of Sustainability and Environmental Management*, *2*(4), 241–256. https://doi.org/10.3126/josem.v2i4.61026

Beckline, M., Mukete, N., and Mukete, T. (2025). *Impact of extreme weather events on agricultural production and household livelihoods in rural Malawi*. 1–12.

Bilalam Jabik, B. (2021). The Agonies of Covid 19 on Vegetable Farmers Along the White Volta River Basin in the Upper East Region of Ghana. *International Journal of Managing Value and Supply Chains*, *12*(03), 1–8. https://doi.org/10.5121/ijmvsc.2021.12301

Dahan, K. S., Kasei, R. A., and Husseini, R. (2023). Land use land cover (LULC) degradation intensity analysis of Guinea savannah and mosaic Forest savannah zones in Ghana. *All Earth*, *35*(1), 302–328. https://doi.org/10.1080/27669645.2023.2255443

Diba, I., Camara, M., Sarr, A. B., and Diedhiou, A. (2018). Potential impacts of land cover change on the interannual variability of rainfall and surface temperature over West Africa. *Atmosphere*, *9*(10). https://doi.org/10.3390/atmos9100376

Dibaba, W. T., Demissie, T. A., and Miegel, K. (2020). Watershed hydrological response to combined land use/land cover and climate change in highland Ethiopia: Finchaa catchment. *Water (Switzerland)*, *12*(6). https://doi.org/10.3390/w12061801

Dzebre, D. E. K., Asiedu, C., Akowuah, E., Boahen, S., Amoabeng, K. O., and Oppong, D. (2024). An Assessment of the impacts of selected Meteorological and land use/land cover datasets on the accuracy of wind speeds downscaled with the Weather Research and Forecasting Model for coastal areas in Ghana. *Journal of Renewable Energies*, *27*(1), 99–114. https://doi.org/10.54966/jreen.v27i1.1162

Edward Adiibokah, A. details. (2020). University for Development Studies, Tamale. *Medical J*, 255973. www.udsspace.uds.edu.gh

Emlaei, Z., Pourebrahim, S., Heidari, H., and Lee, K. E. (2022). The Impact of Climate Change as Well as Land-Use and Land-Cover Changes on Water Yield Services in Haraz Basin. *Sustainability (Switzerland)*, *14*(13). https://doi.org/10.3390/su14137578

Fagariba, C. J., Song, S., and Baoro, S. K. G. S. (2018). Climate change adaptation strategies and constraints in Northern Ghana: Evidence of farmers in Sissala West District. *Sustainability (Switzerland)*, *10*(5), 1–18. https://doi.org/10.3390/su10051484

Fonte, C. C., See, L., Laso-Bayas, J. C., Lesiv, M., and Fritz, S. (2020). Assessing the accuracy of land use land cover (LULC) maps using class proportions in the reference data. *ISPRS Annals of the Photogrammetry, Remote Sensing and Spatial Information Sciences*, *5*(3), 669–674. https://doi.org/10.5194/isprs-Annals-V-3-2020-669-2020

1003 Frimpong, B. F., Koranteng, A., and Opoku, F. S. (2023). Analysis of urban expansion and its
1004 impact on temperature utilising remote sensing and GIS techniques in the Accra
1005 Metropolis in Ghana (1986–2022). *SN Applied Sciences*, *5*(8).
1006 https://doi.org/10.1007/s42452-023-05439-z

1007 Frimpong, K., Eugene Atiemo, D., and Van Etten, E. J. (2022). Urban sprawl and microclimate
1008 in the Ga East municipality of Ghana. *Heliyon*, *8*(7), e09791.
1009 https://doi.org/10.1016/j.heliyon.2022.e09791

1010 Gabiri, G., Diekkrüger, B., Näschen, K., Leemhuis, C., van der Linden, R., Mwanjalolo
1011 Majaliwa, J. G., and Obando, J. A. (2020). Impact of Climate and Land Use / Land Cover
1012 Change on the Water Resources of a Tropical Inland Valley. *Climate*, *83*(8), 1–25.

1013 Galata, A. W., Demissei, T. A., and Leta, M. K. (2020). Watershed Hydrological Responses to
1014 Changes in Land Use and Land Cover at Hangar Watershed, Ethiopia. *Iranian Journal of*
1015 *Energy and Environment*, *11*(1), 1–7. https://doi.org/10.5829/ijee.2020.11.01.01

1016 Gashaw, T., Tulu, T., Argaw, M., and Worqlul, A. W. (2018). Modeling the hydrological
1017 impacts of land use/land cover changes in the Andassa watershed, Blue Nile Basin,
1018 Ethiopia. *Science of the Total Environment*, *619–620*, 1394–1408.
1019 https://doi.org/10.1016/j.scitotenv.2017.11.191

1020 Gautam, L., and Rai, R. (2022). Land Use and Land Cover Change Analysis Using Google
1021 Earth Engine in Manamati Watershed of Kathmandu District, Nepal. *The Third Pole:*
1022 *Journal of Geography Education*, *22*(1995), 49–60.
1023 https://doi.org/10.3126/ttp.v22i01.52560

1024 Gross, E., and Pennink, C. (2018). *Impact Evaluation of the Sustainable Water Fund (FDW)*
1025 *Integrated Water Management and Knowledge Transfer in Sisili Kulpawn Basin (FDW /*
1026 *12 / GH / 02) in the Northern Region of Ghana Final report December 2018*. *December*,
1027 1–71.

1028 Gudmann, A., Csikós, N., Szilassi, P., and Mucsi, L. (2020). Improvement in satellite image-
1029 based land cover classification with landscape metrics. *Remote Sensing*, *12*(21), 1–21.
1030 https://doi.org/10.3390/rs12213580

1031 Guug, S. S., Abdul-Ganiyu, S., and Kasei, R. A. (2020). Application of SWAT hydrological
1032 model for assessing water availability at the Sherigu catchment of Ghana and Southern
1033 Burkina Faso. *HydroResearch*, *3*, 124–133. https://doi.org/10.1016/j.hydres.2020.10.002

1034 Gyimah, A. B. K., Bagbohouna, M., Sanogo, N. dit M., & Gibba, A. (2020). Climate Change
1035 Adaptation among Smallholder Farmers: Evidence from Ghana. *Atmospheric and Climate*
1036 *Sciences*, *10*(04), 614–638. https://doi.org/10.4236/acs.2020.104032

1037 Hyandye, C. B., Worqul, A., Martz, L. W., and Muzuka, A. N. N. (2018). The impact of future
1038 climate and land use/cover change on water resources in the Ndembera watershed and
1039 their mitigation and adaptation strategies. *Environmental Systems Research*, *7*(1).
1040 https://doi.org/10.1186/s40068-018-0110-4

1041 Idrissou, M., Diekkrüger, B., Tischbein, B., de Hipt, F. O., Näschen, K., Poméon, T., Yira, Y.,
1042 and Ibrahim, B. (2022). Modeling the Impact of Climate and Land Use/Land Cover
1043 Change on Water Availability in an Inland Valley Catchment in Burkina Faso. *Hydrology*,
1044 *9*(1). https://doi.org/10.3390/hydrology9010012

1045 Issahaku, A.-R. (2023). Impacts of Climate Change, Land Use and Land Cover Changes on

Watersheds in the Upper East Region of Ghana. *Journal of Geography, Environment and Earth Science International*, *27*(3), 33–44. https://doi.org/10.9734/jgeesi/2023/v27i3673

Jaiswal, T., and Jhariya, D. C. (2020). Impacts of Land Use Land Cover Change on Surface Temperature and Groundwater Fluctuation in Raipur District. *Journal of the Geological Society of India*, *95*(4), 393–402. https://doi.org/10.1007/s12594-020-1448-6

Kassaye, S. M., Tadesse, T., Tegegne, G., and Hordofa, A. T. (2024). Quantifying the climate change impacts on the magnitude and timing of hydrological extremes in the Baro River Basin, Ethiopia. *Environmental Systems Research*, *13*(1), 1–15. https://doi.org/10.1186/s40068-023-00328-1

Kenea, U., Adeba, D., Regasa, M. S., and Nones, M. (2021). Hydrological responses to land use land cover changes in the fincha'a watershed, Ethiopia. *Land*, *10*(9), 1–23. https://doi.org/10.3390/land10090916

Kibii, J. K., Kipkorir, E. C., and Kosgei, J. R. (2021). Application of soil and water assessment tool (SWAT) to evaluate the impact of land use and climate variability on the Kaptagat catchment river discharge. *Sustainability (Switzerland)*, *13*(4), 1–19. https://doi.org/10.3390/su13041802

Kimbi, S. B., Onodera, S., Wang, K., Kaihotsu, I., and Shimizu, Y. (2024). Assessing the Impact of Urbanization and Climate Change on Hydrological Processes in a Suburban Catchment. *Environments*, *11*(10), 225. https://doi.org/10.3390/environments11100225

Kosoe, E. A., and Ahmed, A. (2022). Climate change adaptation strategies of cocoa farmers in the Wassa East District: Implications for climate services in Ghana. *Climate Services*, *26*, 100289. https://doi.org/10.1016/J.CLISER.2022.100289

Kouassi, J. L., Gyau, A., Diby, L., Bene, Y., and Kouamé, C. (2021). Assessing land use and land cover change and farmers' perceptions of deforestation and land degradation in south-west Côte d'Ivoire, West Africa. *Land*, *10*(4). https://doi.org/10.3390/land10040429

Kuma, H. G., Feyessa, F. F., and Demissie, T. A. (2021). Hydrologic responses to climate and land-use/land-cover changes in the Bilate catchment, southern Ethiopia. *Journal of Water and Climate Change*, *12*(8), 3750–3769. https://doi.org/10.2166/wcc.2021.281

Kumah, M., Abagale, F. K., and Baatuuwie, B. N. (2026). Heliyon Impact of land use and land cover change on the Nasia River catchment hydrology. *Heliyon*, *12*(4), e44743. https://doi.org/10.1016/j.heliyon.2026.e44743

Kwawuvi, D., Mama, D., Agodzo, S. K., Bessah, E., Yangouliba, G. I., and Aklamati, W. S. (2023). Potential consequences for rising temperature trends in the Oti River Basin, West Africa. *Frontiers in Climate*, *5*. https://doi.org/10.3389/fclim.2023.1184050

Kwawuvi, D., Mama, D., Agodzo, S. K., Hartmann, A., Larbi, I., Bessah, E., Limantol, A. M., Dotse, S. Q., Yangouliba, G. I. (2022). Spatiotemporal variability and change in rainfall in the Oti River Basin, West Africa. *Journal of Water and Climate Change*, *13*(3), 1151–1169. https://doi.org/10.2166/wcc.2022.368

Li, C., Dash, J., Asamoah, M., Sheffield, J., Dzodzomenyo, M., Gebrechorkos, S. H., Anghileri, D., and Wright, J. (2022). Increased flooded area and exposure in the White Volta River basin in Western Africa, identified from multi-source remote sensing data. *Scientific Reports*, *12*(1), 1–13. https://doi.org/10.1038/s41598-022-07720-4

Li, W., Li, L., Chen, J., Lin, Q., and Chen, H. (2021). Impacts of land use and land cover

change and reforestation on summer rainfall in the Yangtze River basin. *Hydrology and Earth System Sciences*, *25*(8), 4531–4548. https://doi.org/10.5194/hess-25-4531-2021

Liu, J., Yi, Z., Fang, Y., and Wu, C. (2024). Ecological Vulnerability Assessment of the Three Rivers Source Area Based on the Analytic Hierarchy Process. *Water (Switzerland)*, *16*(14). https://doi.org/10.3390/w16142023

Lukas, P., Melesse, A. M., and Kenea, T. T. (2025). Integrating Land Use/Land Cover and Climate Change Projections to Assess Future Hydrological Responses: A CMIP6-Based Multi-Scenario Approach in the Omo–Gibe River Basin, Ethiopia. *Climate*, *13*(3). https://doi.org/10.3390/cli13030051

Malede, D. A., Alamirew, T., and Andualem, T. G. (2023). Integrated and Individual Impacts of Land Use Land Cover and Climate Changes on Hydrological Flows over Birr River Watershed, Abbay Basin, Ethiopia. *Water (Switzerland)*, *15*(1). https://doi.org/10.3390/w15010166

Mekonnen, Y. A., and Manderso, T. M. (2023). Land use/land cover change impact on streamflow using Arc-SWAT model, in case of Fetam watershed, Abbay Basin, Ethiopia. *Applied Water Science*, *13*(5), 1–19. https://doi.org/10.1007/s13201-023-01914-5

Mengistu, A. G., Woldesenbet, T. A., Dile, Y. T., Bayabil, H. K., and Tefera, G. W. (2023). Modeling impacts of projected land use and climate changes on the water balance in the Baro basin, Ethiopia. *Heliyon*, *9*(3), e13965. https://doi.org/10.1016/j.heliyon.2023.e13965

Mensah, J. K., Ofosu, E. A., Akpoti, K., Kabo-Bah, A. T., Okyereh, S. A., and Yidana, S. M. (2022). Modeling current and future groundwater demands in the White Volta River Basin of Ghana under climate change and socio-economic scenarios. *Journal of Hydrology: Regional Studies*, *41*(January), 101117. https://doi.org/10.1016/j.ejrh.2022.101117

Mensah, J. K., Ofosu, E. A., Yidana, S. M., Akpoti, K., and Kabo-bah, A. T. (2022). Integrated modeling of hydrological processes and groundwater recharge based on land use land cover, and climate change: A systematic review. *Environmental Advances*, *8*(March), 100224. https://doi.org/10.1016/j.envadv.2022.100224

Minallah, N., Khan, Z. N., Rashid, A. U., and Khan, K. Z. (2019). Classification and Evaluation of Land Cover Variations Using Landsat Data. *J. Inf. Commun. Technol. Robot. Appl*, *10*(2), 18–24.

Moisa, M. B., Dejene, I. N., Hinkosa, L. B., and Gemeda, D. O. (2022). Land use/land cover change analysis using geospatial techniques: a case of Geba watershed, western Ethiopia. *SN Applied Sciences*, *4*(6). https://doi.org/10.1007/s42452-022-05069-x

Mortey, E. M., Arnault, J., Inoussa, M. M., Madougou, S., Annor, T., Laux, P., Dieng, M. D. B., and Kunstmann, H. (2024). Regional climate response to land cover change in tropical West Africa: a numerical sensitivity experiment with ESA land cover data and advanced WRF-Hydro. *Frontiers in Water*, *6*(July). https://doi.org/10.3389/frwa.2024.1372333

Murtaza, K. O., Shafai, S., Shahid, P., and Romshoo, S. A. (2023). Understanding the linkages between spatio-temporal urban land system changes and land surface temperature in Srinagar City, India, using image archives from Google Earth Engine. *Environmental Science and Pollution Research*, *30*(49), 107281–107295. https://doi.org/10.1007/s11356-023-28889-9

Mustapha, U. F., Akongyuure, D. N., Abagale, F. K., and Alhassan, E. H. (2016). Fish and fisheries of the Sisili-Kulpawn river basin in the Northern region , Ghana. *Journal of Biodiversity and Environmental Sciences (JBES)*, *9*(March), 112–119. https://innspub.net/jbes/fish-and-fisheries-of-the-sisili-kulpawn-river-basin-in-the-northern-region-ghana/

Mwanga, E., Shaibu, A. G., and Issaka, Z. (2024). Assessing the impact of land use and land cover (LULC) changes on the surface runoff downstream of an ungauged Bontanga watershed in Northern Ghana. *Water Practice and Technology*, *19*(4), 1348–1364. https://doi.org/10.2166/wpt.2024.061

Naazie, G. K., Dakyaga, F., and Derbile, E. K. (2023). Agro-ecological intensification for climate change adaptation: tales on soil and water management practices of smallholder farmers in rural Ghana. *Discover Sustainability*, *4*(1). https://doi.org/10.1007/s43621-023-00142-w

Nasare, L. I., Opoku, S. A., Amponsah, A., Tom-Dery, D., Asante, W. J., and Baatuuwie, B. N. (2023). Effect of sand mining on riparian landcover transformation in Dallung-Kukou catchment of the White Volta basin, Ghana. *Heliyon*, *9*(8), e18428. https://doi.org/10.1016/j.heliyon.2023.e18428

Ngondo, J., Mango, J., Nobert, J., Dubi, A., Li, X., and Cheng, H. (2022). Hydrological Response of the Wami-Ruvu Basin to Land-Use and Land-Cover Changes and Its Impacts for the Future. *Water (Switzerland)*, *14*(2). https://doi.org/10.3390/w14020184

Nigusie, A., and Dananto, M. (2021). Impact of land use/land cover change on hydrologic processes in Dijo watershed, central rift valley, Ethiopia. *International Journal of Water Resources and Environmental Engineering*, *13*(1), 37–48. https://doi.org/10.5897/IJWREE2020.0956

Nsiah, J. J., Gyamfi, C., Anornu, G. K., and Odai, S. N. (2021). Estimating the spatial distribution of evapotranspiration within the Pra River Basin of Ghana. *Heliyon*, *7*(4). https://doi.org/10.1016/j.heliyon.2021.e06828

Nsor, C. A., Ashiagbor, G., and Danquah, E. (2019). Quantifying Recent Floodplain Vegetation Change along the White Volta River in the Northern Region of Ghana. *Ghana Journal of Geography*, *11*(1), 159–179.

Nyadzi, E., Bessah, E., Kranjac-Berisavljevic, G., and Ludwig, F. (2021). Hydro-climatic and land use/cover changes in Nasia catchment of the White Volta basin in Ghana. *Theoretical and Applied Climatology*, *146*(3–4), 1297–1314. https://doi.org/10.1007/s00704-021-03772-0

Nyarko, B. K. (2020). Wetland River Flow Interaction in a Sedimentary Formation of the White Volta Basin of Ghana. *Earth Science Research*, *9*(1), 15. https://doi.org/10.5539/esr.v9n1p15

Nyatuame, M., Amekudzi, L. K., and Agodzo, S. K. (2020). Assessing the land use/land cover and climate change impact on water balance on Tordzie watershed. *Remote Sensing Applications: Society and Environment*, *20*(August), 100381. https://doi.org/10.1016/j.rsase.2020.100381

O'Neill, B. C., Carter, T. R., Ebi, K., Harrison, P. A., Kemp-Benedict, E., Kok, K., Kriegler, E., Preston, B. L., Riahi, K., Sillmann, J., van Ruijven, B. J., van Vuuren, D., Carlisle, D., Conde, C., Fuglestvedt, J., Green, C., Hasegawa, T., Leininger, J., Monteith, S., and Pichs-

Madruga, R. (2021). Publisher Correction: Achievements and needs for the climate change scenario framework (Nature Climate Change, 2020, 10, 12, (1074-1084), 10.1038/s41558-020-00952-0). *Nature Climate Change*, *11*(3), 274. https://doi.org/10.1038/s41558-020-00981-9

O'Neill, B. C., Kriegler, E., Ebi, K. L., Kemp-Benedict, E., Riahi, K., Rothman, D. S., van Ruijven, B. J., van Vuuren, D. P., Birkmann, J., Kok, K., Levy, M., and Solecki, W. (2017). The roads ahead: Narratives for shared socioeconomic pathways describing world futures in the 21st century. *Global Environmental Change*, *42*, 169–180. https://doi.org/10.1016/j.gloenvcha.2015.01.004

Okrah, A., Prempeh, N. A., Mensah, C., John, R., Kumi, N., Otu-larbi, F., and Kyere-boateng, R. (2020). *Impact of Spatio-Temporal Land Cover Changes on Land Surface Temperature over Dormaa from 1990- 2020*. *6*(4).

Osman, Z., Gyamfi, C., Ofosu, S. A., and Baatuuwie N.B (2025). Effects of Land Cover Changes on Ecosystem Services in the Kulpawn Catchment of the White Volta River Basin of Ghana. *Available at SSRN …*, *6*(6), 100277. https://doi.org/10.1016/j.regsus.2025.100277

Oti, E. A. (2024). Assessment Of Drivers Of Rainfall Variability In The Northern Assessment Of Drivers Of Rainfall Variability In. *August*. https://doi.org/10.13140/RG.2.2.30944.70405

Ougahi, J. H., Karim, S., and Mahmood, S. A. (2022). Application of the SWAT model to assess climate and land use/cover change impacts on water balance components of the Kabul River Basin, Afghanistan. *Journal of Water and Climate Change*, *13*(11), 3977–3999. https://doi.org/10.2166/wcc.2022.261

Pabi, O., Egyir, S., and Attua, E. M. (2021). Flood hazard response to scenarios of rainfall dynamics and land use and land cover change in an urbanized river basin in Accra, Ghana. *City and Environment Interactions*, *12*, 100075. https://doi.org/10.1016/j.cacint.2021.100075

Peters, M. K. (2019). *Assessing Land Use and Land Cover Change in the Keta Municipality of Ghana Using Remote Sensing*. *10343535*, 104. http://ugspace.ug.edu.gh/bitstream/handle/123456789/32954/Assessing Land Use and Land Cover Change in the Keta Municipality of Ghana Using Remote Sensing.pdf?sequence=1&isAllowed=y

Rivas-Tabares, D., Tarquis, A. M., De Miguel, Á., Gobin, A., & Willaarts, B. (2022). Enhancing LULC scenarios impact assessment in hydrological dynamics using participatory mapping protocols in semiarid regions. *Science of the Total Environment*, *803*, 149906. https://doi.org/10.1016/j.scitotenv.2021.149906

Sambe, L. N., Adeofun, C. O., Oyedepo, J. A., Osunmadewa, B. A., Jande, J. A., and Land, M. (2025). *Multi-Temporal Land Use and Land Cover Change Detection in Northern Nigeria's Frontline States : Geospatial Insights for Sustainable Development and Climate Adaptation Multi-Temporal Land Use and Land Cover Change Detection in Northern Nigeria's Front*.

Savargiv, M., Masoumi, B., and Keyvanpour, M. R. (2021). A new random forest algorithm based on learning automata. *Computational Intelligence and Neuroscience*, *2021*. https://doi.org/10.1155/2021/5572781

Sisay, G., Gitima, G., Mersha, M., and Alemu, W. G. (2021). Assessment of land use land cover dynamics and its drivers in Bechet Watershed Upper Blue Nile Basin, Ethiopia. *Remote Sensing Applications: Society and Environment*, *24*(September). https://doi.org/10.1016/j.rsase.2021.100648

Stewart, R. H., Hu, C. H., Ran, G., Li, G., Yu, Y., Wu, Q., Yan, D., Jian, S., Tiwari, J., Sharma, S. K., Patil, R. ., Aznarez, C., Jimeno-Sáez, P., López-Ballesteros, A., Pacheco, J. P., Senent-Aparicio, J., Diba, I., Camara, M., Sarr, A. B., … Wang, S. L. S. S. (2021). Land-Use / Land Cover Change And Its Relationship To Changing Climate And Crop Production In The Lower Volta Basin, Ghana. University of Ghana. http://ugspace.ug.edu.gh DECLARATION. *Climate*, *12*(1), 1–18. https://doi.org/10.7717/peerj.7523

Tahiru, A. A., Doke, D. A., and Baatuuwie, B. N. (2020). Effect of land use and land cover changes on water quality in the Nawuni Catchment of the White Volta Basin, Northern Region, Ghana. *Applied Water Science*, *10*(8), 1–14. https://doi.org/10.1007/s13201-020-01272-6

Takayama, R., Nakamura, R., Esteban, M., Mäll, M., and Ohizumi, K. (2023). Pseudo global warming experiment of flood inundation in the upper White Volta River, Ghana. *Journal of Hydrology: Regional Studies*, *45*, 101297. https://doi.org/10.1016/J.EJRH.2022.101297

Tan, K. C., Lim, H. S., MatJafri, M. Z., and Abdullah, K. (2010). Landsat data to evaluate urban expansion and determine land use/land cover changes in Penang Island, Malaysia. *Environmental Earth Sciences*, *60*(7), 1509–1521. https://doi.org/10.1007/s12665-009-0286-z

Tan, M. L., Ibrahim, A. L., Yusop, Z., Duan, Z., and Ling, L. (2015). Impacts of land-use and climate variability on hydrological components in the Johor River basin, Malaysia. *Hydrological Sciences Journal*, *April 2015*, 1–17. https://doi.org/10.1080/02626667.2014.967246

Tengapoe, K., Baddianaah, I., and Agyemang, I. (2023). Anthropogenic-induced land use land cover dynamics of the Black Volta River Corridor in north-western Ghana, 2011-2021. *Trees, Forests and People*, *14*(September), 100449. https://doi.org/10.1016/j.tfp.2023.100449

Thrasher, B., Wang, W., Michaelis, A., Melton, F., Lee, T., and Nemani, R. (2022). NASA Global Daily Downscaled Projections, CMIP6. *Scientific Data*, *9*(1), 1–6. https://doi.org/10.1038/s41597-022-01393-4

Timilsina, S., Shrestha, S., Tripathi, S., and Bhattarai, R. (2023). *Eurasian Journal of Soil Science Assessment of land use land cover dynamics and its impact on*. *12*(x), 1–15.

Tola, B., and Deyassa, G. (2024). A modeling approach for evaluating and predicting the impacts of land use land cover changes on groundwater recharge in Walga Watershed, Upper Omo Basin, Central Ethiopia. *Journal of Hydrology: Regional Studies*, *51*(January), 101659. https://doi.org/10.1016/j.ejrh.2024.101659

Tumsa, B. C., Kenea, G., and Tola, B. (2022). The application of SWAT+ model to quantify the impacts of sensitive LULC changes on water balance in Guder catchment, Oromia, Ethiopia. *Heliyon*, *8*(12), e12569. https://doi.org/10.1016/j.heliyon.2022.e12569

Umukiza, E., Abagale, F. K., and Adongo, T. A. (2024). Characterization of land use and land

cover dynamics and their impact on runoff generation patterns in dam catchments of Northern Ghana. *Geocarto International*, *39*(1). https://doi.org/10.1080/10106049.2024.2335247

Yeneneh, N., Elias, E., and Feyisa, G. L. (2022). Detection of land use/land cover and land surface temperature change in the Suha Watershed, North-Western highlands of Ethiopia. *Environmental Challenges*, *7*. https://doi.org/10.1016/j.envc.2022.100523

Yenibehit, N., Abdulai, A., Amikuzuno, J., and Blay, J. K. (2024). Impacts of farming and herding activities on land use and land cover changes in the north eastern corridor of Ghana: A comprehensive analysis. *Sustainable Environment*, *10*(1). https://doi.org/10.1080/27658511.2024.2307229

Supplementary Files

This is a list of supplementary files associated with this preprint. Click to download.

- Keyhighlights.pdf